# Dalton Transactions

Accepted Manuscript






ROYAL SOCIETY OF CHEMISTRY

www.rsc.org/dalton

General synthetic protocols for well-defined organometallic compounds of heavy pnicogens with the pincer group, 2,6-$[MeN(CH_2CH_2)_2NCH_2]_2C_6H_3$, and oxo ligands are reported.

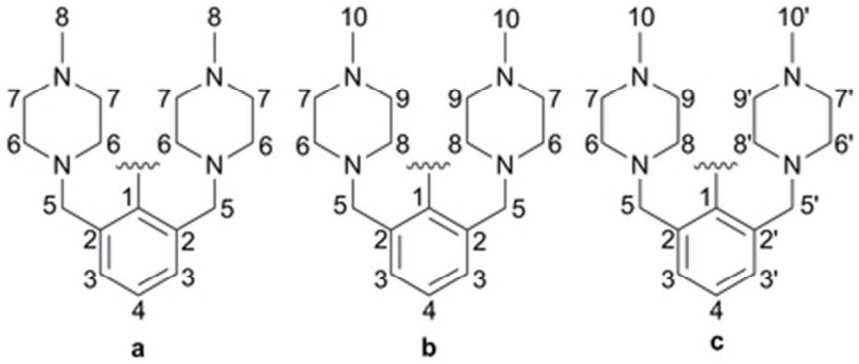


36x15mm (300 x 300 DPI)

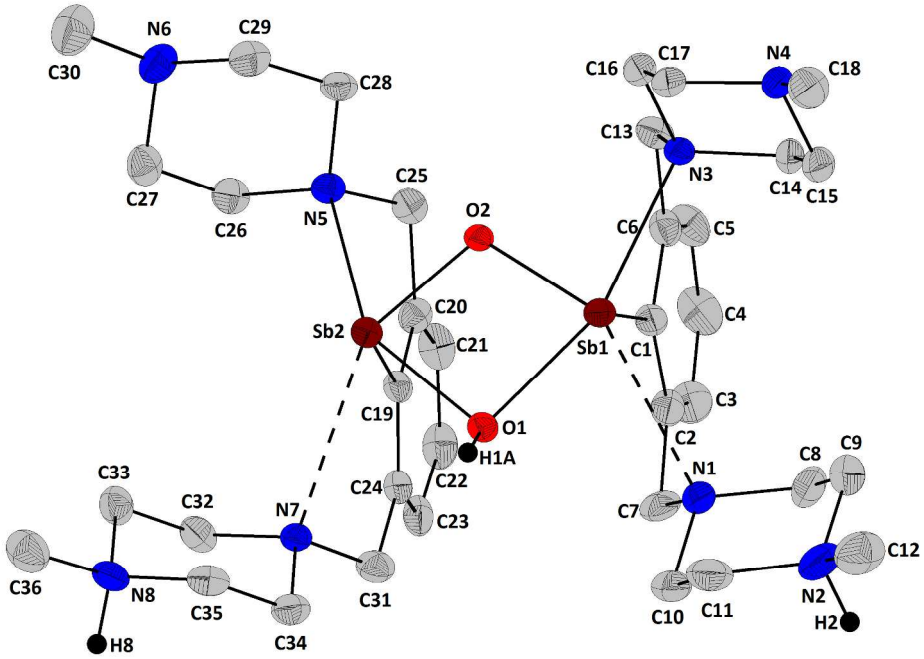


635x423mm (120 x 120 DPI)

Journal Name

RSCPublishing

ARTICLE

# A general route to monoorganopnicogen(III) (M = Sb, Bi) compounds with a pincer (*N,C,N*) group and oxo ligands

Cite this: DOI: 10.1039/x0xx00000x

Received 00th January 2012,
Accepted 00th January 2012

DOI: 10.1039/x0xx00000x

www.rsc.org/

Gabriela Strîmb, Alpár Pöllnitz, Ciprian I. Raţ and Cristian Silvestru

The reaction of $RMCl_2$ [R = 2,6-[$MeN(CH_2CH_2)_2NCH_2]_2C_6H_3$; M = Sb (**1**), Bi (**2**)] with KOH affords the isolation of the oxides *cyclo*-$R_2M_2O_2$ [M = Sb (**3**), Bi (**4**)]. Treatment of **3** with trifluoroacetic acid produced an ionic species (**5**) with a dinuclear cation that contains organic ligands protonated partially at one of the pendant arms. The cyclic oxides **3** and **4** are able to trap gaseous $CO_2$ to give "$RMCO_3$" [M = Sb (**6**), Bi (**7**)], the degree of these organometallic carbonates oligomerization being under investigation. The reactivity of the dinuclear oxide **3** was also investigated towards oxalic acid or dopamine hydrochloride and pure mononuclear compounds could be isolated, *i.e.* RSb[O(O)CC(O)O] (**8**) and RSb[$O_2$-1,2-$C_6H_3$-3-$(CH_2)_2NH_3$]Cl (**9**). The reaction of the dichlorides **1** and **2** with ethylene glycol, pinacol or catechol, in presence of KOH, led to 2-organo-1,3,2-dioxastibolanes or -bismolanes $RM(OCH_2)_2$ [M = Sb (**10**), Bi (**11**)], $RM(OCMe_2)_2$ [M = Sb (**12**), Bi (**13**)] and 2-organo-1,3,2-dioxastibole or -bismole $RM(O_2$-1,2-$C_6H_4)$ [M = Sb (**14**), Bi (**15**)], respectively. The compounds were investigated by NMR spectroscopy, including variable temperature experiments, providing evidences for the presence of the intramolecular N→M interactions in solution. Single crystal X-ray diffraction studies were performed for most compounds and revealed an organic group R acting as a pincer ligand resulting in a distorted square pyramidal (*N,C,N*)$MO_2$ core with *cis* intramolecular N→M interactions placed in *trans* to M–O bonds. This contrasts to the N→M interactions *trans* to each other as found in the $RMCl_2$ used as starting materials. The crystals of the oxides **3** and **4**·$4H_2O$ contain different geometric isomers with *anti* and *syn* orientation of the M–C bonds, respectively, with respect to the planar $M_2O_2$ ring. In the supramolecular polymeric architecture established in the crystal of **4**·$4H_2O$ an important finding is the experimental observation of water hexamer units with a [tetramer+2] structure (water molecules connected to opposite corners of a square water tetramer) fixed between 1D-chains of the type (*syn*-$R_2Bi_2O_2·H_2O)_n$ through additional hydrogen bonds to oxygen atoms of the dinuclear organobismuth(III) moieties. Theoretical calculations were carried out on **2**-**6** and **8**-**15** in order to bring insight in the stabilization energy brought by intramolecular coordination of the pendant arms, association degrees and formation energies of the organopnicogen compounds with chelating ligands.

## Introduction

Hypervalent organometallic compounds of heavy pnicogens (antimony, bismuth) were found to have various applications, *e.g.* specific reagents in organic synthesis, catalysts for the preparation of molecular compounds or polymerization processes, etc.[1] Outstanding results were obtained with organopnicogen oxides, alkoxides and aryloxides which were proved to be excellent candidates for the fixation of $CO_2$ when used either as stoichiometric reagents[2-5] or as catalysts.[6-10] While the hypervalent organoantimony(III) oxide *cyclo*-[2,6-$(Me_2NCH_2)_2C_6H_3]_2Sb_2O_2$ was reported to bind reversibly equimolar amounts of $CO_2$ to form the mononuclear carbonate [2,6-$(Me_2NCH_2)_2C_6H_3]SbCO_3$ (Chart 1, **a**),[4] the organoantimony(V) oxide $Ph_3SbO$ was found to be a quite efficient catalyst in the synthesis of cyclic carbonates from epoxides and $CO_2$,[6] as well as the synthesis of linear or cyclic ureas from amines and carbon dioxide.[7] Hypervalent organobismuth(III) oxides, hydroxides and alkoxides, similarly to their organoantimony analogues, have shown to absorb and

reversibly bind stoichiometric amounts of carbon dioxide forming the corresponding carbonates.[2,3] The bismuth complex [2,6-$(Me_2NCH_2)_2C_6H_3$]Bi($C_6H_2{}^tBu_2$-3,5-O-4) (Chart 1, **b**) containing the unusual dianionic $(C_6H_2{}^tBu_2\text{-}3,5\text{-}O\text{-}4)^{2-}$ was prepared from [2,6-$(Me_2NCH_2)_2C_6H_3$]$BiCl_2$ and $KOC_6H_3{}^tBu_2$-2,6.[11] The rearrangement leading to this type of C–H bond activation was a consequence of the facile homolytic cleavage of the Bi–O bond in the corresponding organobismuth(III) di(aryloxide),[11] a behaviour which is also a key step in the mechanism of the SOHIO process.[12-15] The unique species [2,6-$(Me_2NCH_2)_2C_6H_3$]Bi($C_6H_2{}^tBu_2$-3,5-O-4) has been shown to chemically bind $CO_2$ by insertion into the Bi-C bond in the position 4 of the aromatic dianion to produce the carboxylate [2,6-$(Me_2NCH_2)_2C_6H_3$]Bi[$O_2C(C_6H_2{}^tBu_2$-3,5-O-4)-$\kappa^2O,O'$] (Chart 1, **c**).[5,10] Applications of organobismuth(III) compounds in catalytic $CO_2$ fixation have been developed based on these findings. Thus, the dichloride [2,6-$(Me_2NCH_2)_2C_6H_3$]$BiCl_2$,[16,17] has successfully been used as a catalyst in the preparation of 3,5-di-*tert*-butyl-4-hydroxybenzoic acid from 2,6-di-*tert*-butylphenol and $CO_2$.[10]

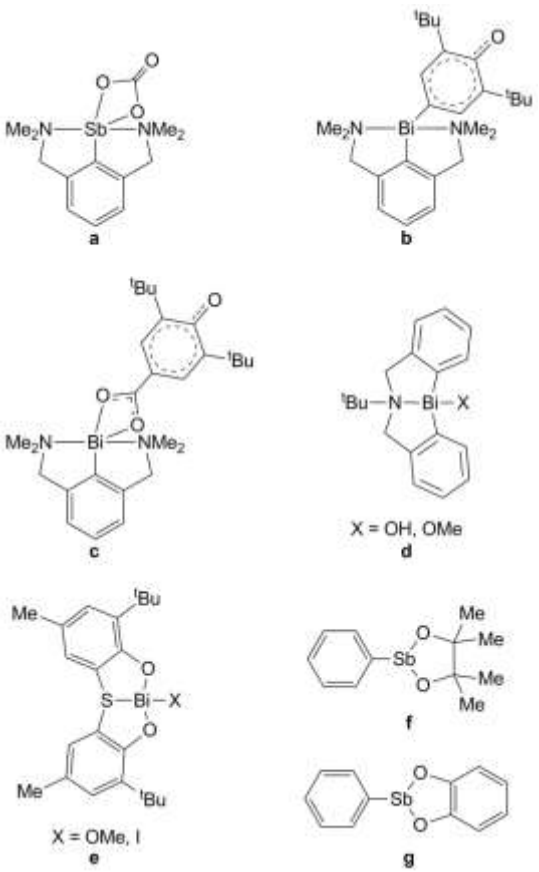


Chart 1 Depiction of the compounds **a** - **g**.

Similarly, following the stoichiometric reactions of $CO_2$ with several hypervalent compounds containing the 5,6,7,12-tetrahydrodibenz[c,f][1,5]azabismocine framework (Chart 1, **d**),[3] the corresponding binuclear organobismuth(III) oxide and sulphide were reported to show high catalytic efficiency in the synthesis of cyclic carbonates from epoxides and $CO_2$.[9] Also, related inorganic 2,2′-thiobis(6-*tert*-butyl-4-methylphenolato)bismuth(III) species (Chart 1, **e**), in the presence of iodide salts as co-catalysts, were found to show high catalytic activity and selectivity for solvent-free synthesis of cyclic propylene carbonate from $CO_2$ and propylene oxide at room temperature.[8]

Several 2-organo-1,3,2-dioxastibolanes (*e.g.* **f** in Chart 1) and -stiboles (*e.g.* **g** in Chart 1) with small substituents on antimony (*i.e.* Me, $^t$Bu, Ph) were prepared by the reaction of 1,2-dihydroxy derivatives with organoantimony(III) dichloride, in presence of $Et_3N$,[18] or by transesterification using $RSb(OEt)_2$ (R = Me, $^t$Bu).[19,20] With exception of $^t$BuSb$(OCH_2)_2$ and $^t$BuSb$(OCMe_2)_2$, for which monomeric species were established by cryoscopic methods,[20] most of these compounds are insoluble polymers which decompose without melting. The reaction of $MesSbCl_2$ with disodium 3,5-di-*tert*-butylcatecholate also gave the corresponding soluble 2-mesityl-1,3,2-dioxastibolane.[21] Using transesterification reactions the related 1,3,2-dioxabismolanes and -bismoles with a methyl group on bismuth were also obtained as insoluble, air and moisture sensitive polymers.[22] To the best of our knowledge, no molecular structure was established by crystallographic methods for such heavy pnicogen(III)-containing organometallic heterocycles, nor they were used in $CO_2$ activation studies.

We report here on the synthesis and characterization of hypervalent heavy organopnicogen(III) compounds containing 2,6-$[MeN(CH_2CH_2)_2NCH_2]_2C_6H_3$ as a pincer (*N,C,N*) group and oxo ligands, including their molecular structure established by single-crystal X-ray diffraction. Since related organopnicogen(III) compounds with oxo ligands proved to be efficient in catalytic $CO_2$ fixation, the title compounds might be appropriate for use in tests for $CO_2$ activation.

## Results and discussion

### Synthetic procedure and characterization

The organoantimony(III) dichloride $RSbCl_2$ (**1**) (R = 2,6-$[MeN(CH_2CH_2)_2NCH_2]_2C_6H_3$) was obtained from RLi and $SbCl_3$ in $Et_2O$ using a similar procedure as described for the organobismuth(III) analogue, $RBiCl_2$ (**2**).[23] The dichloride **1** is well soluble in chlorinated solvents, ethanol and even water, but poorly soluble in toluene and acetone. Treatment of $RMCl_2$ with KOH in ethanol or toluene gave the oxides *cyclo*-$R_2M_2O_2$ [M = Sb (**3**), Bi (**4**)]. While the cyclic oxide **3** is stable in solution, the bismuth analogue **4** is practically insoluble in benzene at room temperature and fully decomposes in $CHCl_3$ or $CH_2Cl_2$ within ca. 48 h as suggested by NMR data and the insoluble species which appear in the NMR tube (the resulting products were not identified). At 50 °C the decomposition process of **4** has a higher rate and is completed after ca. 1h. The dinuclear nature was preserved when the oxide **3** was reacted with trifluoroacetic acid and an ionic species,



 

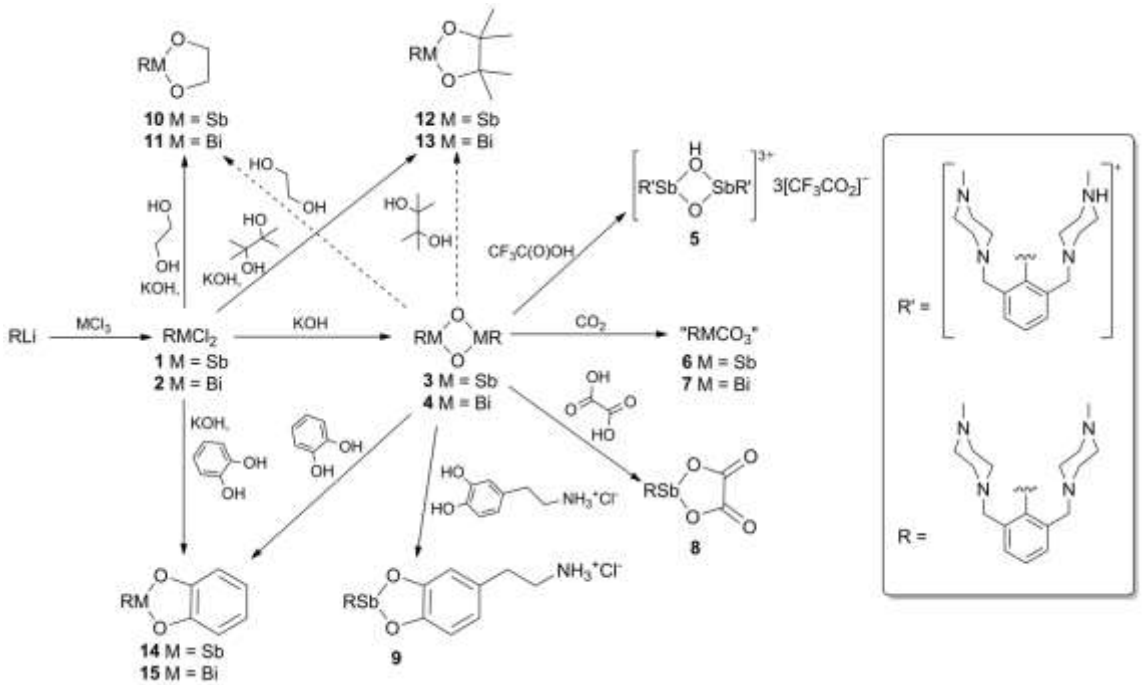


Scheme 1 Depiction of the synthesis of compounds **1** – **15** (dashed arrows indicate NMR tube scale experiments carried out for compounds **10** and **12**).

[*cyclo*-{2-(MeN(H){$CH_2CH_2$}$_2$$NCH_2$)-6-(MeN{$CH_2CH_2$}$_2$$NCH_2$)$C_6H_3$}$_2$$Sb_2O(OH)$]$(O_2CCF_3)_3$ (**5**), was isolated (*vide infra*).

The cyclic oxide **3** exhibits a potential use in the trapping of gaseous $CO_2$. Indeed, a compound characterized as "$RSbCO_3$" (**6**) was isolated when a stream of $CO_2$ was passed for 3 h through a solution of the oxide **3** in $CHCl_3$. During this period the solvent was evaporated leaving pure **6** as a colourless solid, well soluble in $CHCl_3$, $CH_2Cl_2$, methanol and water, poorly soluble in toluene and diethyl ether. The $^1H$ and $^{13}C$ NMR data indicate the presence of only one species in $CDCl_3$ solution (see Figures S22 and S23 in ESI†) and the resonance signal at $\delta$ 161.00 ppm is consistent with the presence of the carbonate unit. The IR spectrum of **6** in KBr pellets shows absorption bands corresponding to the carbonate group at 1700, 1682 and 1644 $cm^{-1}$. Although they seem to be similar to those reported for the monomeric species [2,6-$(Me_2NCH_2)_2C_6H_3$]$SbCO_3$,[4] a dimer association cannot be definitively ruled out. It is worthwhile to mention here that for the analogous organobismuth(III) carbonate a chain polymeric structure, [{2,6-$(Me_2NCH_2)_2C_6H_3$}$BiCO_3$]$_n$, was established in solid state.[24] The carbonate **6** slowly looses $CO_2$ in $CDCl_3$ solution as observed when the $^1H$ NMR spectrum was recorded at 60 °C. After ca. 2 h at 80 °C the $^1H$ NMR spectrum of the same sample indicated the conversion of ca. 80% of the carbonate **6** into the oxide **3**. To prove the reversible capture of $CO_2$ by the oxide **3** the following experiments have been carried out. IR and $^1H$ NMR spectra were recorded for a sample of oxide **3** and for the carbonate **6** obtained from it. Then, part of the sample of **6** was dissolved in $CHCl_3$ and the solution was heated at 70 °C. After 4 h the solvent was removed and the remaining solid was characterized by $^1H$ NMR and IR spectroscopy, indicating the reversible conversion to **3** in solution. A solid sample of carbonate **6** resulted from the same synthesis was heated at 110 °C. After 9 h the complete decomposition of the carbonate sample to the oxide **3** was confirmed by $^1H$ NMR and IR spectroscopy. The IR spectrum of this oxide sample did not show any absorption bands in the range 700–600 $cm^{-1}$ where the Sb=O stretching vibration were reported for $Ph_3SbO$ (668, 660 and 653 $cm^{-1}$)[25] or $Mes_3SbO{\cdot}CF_3SOH$ (700, 675 and 640 $cm^{-1}$).[26] Both oxide samples obtained from the solution and solid state decomposition experiments were separately dissolved in $CHCl_3$, then $CO_2$ was passed through the obtained solutions following the protocol described in Experimental section. Formation of the carbonate was again confirmed by IR and $^1H$ NMR spectroscopy (see Figures S24-S26 in ESI†). The easy conversion of the carbonate 6 into the oxide 3 in solution is in contrast to the behaviour of the related [2,6-$(Me_2NCH_2)_2C_6H_3$]$SbCO_3$ which was reported to be quite stable both in $CHCl_3$ solution and in solid state at room temperature and elimination of $CO_2$ occurred only after heating a solid sample at 130 °C.[4] A thermogravimetric analysis was run on a carbonate sample obtained after a repeated cycle of $CO_2$ absorption/desorption and dried at reduced pressure ($10^{-3}$ mbar) for 1 h at room temperature. The practical mass loss (9.17%) in the interval 100-215 °C is only slightly larger than the theoretical calculated value of 9.1% (see Figure S27 in ESI†). Heating the carbonate **6** at temperatures higher than 215 °C, according to TGA, leads to a significant mass loss which suggests decomposition of the pendant arm ligand as well. It

should be also noted that an attempt to prepare **6** from the dichloride **1** and $Cs_2CO_3$ in methanol, passing a flow of argon through the solution to remove the solvent to dryness, surprisingly afforded only the isolation of the oxide **3**, thus providing further evidence of the easiness of the $CO_2$ elimination from the carbonate **6** prepared *in situ*.

The related organobismuth(III) carbonate, "$RBiCO_3$" (**7**), was obtained using a similar procedure as used for the preparation of **6**, *i.e.* it was formed by passing a stream of $CO_2$ through a solution of oxide **4** in $CHCl_3$ for 2 h. In contrast to its antimony analogue, the carbonate **7** decomposes at temperatures ranging from 60 to 120 °C into multiple species without being reconverted to the oxide **4**. The attempt to obtain **7** from the reaction of the dichloride **2** with $Cs_2CO_3$ (1:1 molar ratio) in $CH_2Cl_2$ failed, only a partial conversion to a new product (1:3.5 based on integrals from the $^1$H NMR spectrum of the reaction mixture) being achieved. Treatment of this reaction mixture in $CH_2Cl_2$ with a saturated $Na_2CO_3$ aqueous solution gave only a complex mixture of products which was not further investigated.

Mononuclear compounds, *i.e.* RSb[O(O)CC(O)O] (**8**) and RSb[$O_2$-1,2-$C_6H_3$-3-$(CH_2)_2NH_3$]Cl (**9**), were easily obtained, in high yields, when the cyclic oxide **3** was treated with oxalic acid or dopamine hydrochloride (Scheme 1). Reaction of **2** with $K_2C_2O_4$ (prepared *in situ* from oxalic acid and KOH) gave a complex mixture of products which was not further investigated.

The facile reaction of the oxide **3** with dopamine hydrochloride and the isolation of **9** as a stable compound triggered our curiosity to further explore the potential use of the chelation effect with various 1,2-dihydroxo ligands. In a quest to find a general route for organopnicogen(III) species from the less common class of 2-organo-1,3,2-dioxastibolanes/bismolanes and -stiboles/bismoles, members of which reported so far are not thoroughly characterized,[18-22] the reactions of **3** with common diols as ethylene glycol, pinacol or catechol were attempted and were found to easily provide the 2-organo-1,3,2-dioxastibolanes RSb$(OCH_2)_2$ (**10**) (at NMR tube scale), RSb$(OCMe_2)_2$ (**12**) (at NMR tube scale), and the 2-organo-1,3,2-dioxastibole RSb($O_2$-1,2-$C_6H_4$) (**14**) (Scheme 1), respectively, within several hours at room temperature (see Figure 49 in ESI† for the reaction of **3** with pinacol to give compound **12**, as monitored by NMR). To further improve the synthesis protocol of these compounds by reducing the number of steps and to extend the general protocol to organobismuth(III) analogous the use of chlorides **1** and **2** as staring materials was envisaged. Indeed, treatment of the dichlorides **1** and **2** with ethylene glycol, pinacol or catechol, in presence of KOH, led to the organoantimony(III) compounds **10**, **12** and **14**, as well as their analogous species RBi$(OCH_2)_2$ (**11**), RBi$(OCMe_2)_2$ (**13**) and RBi($O_2$-1,2-$C_6H_4$) (**15**), respectively.

All compounds were investigated by NMR spectroscopy in solution. The assignment of the $^1$H and $^{13}$C resonance signals was carried out using COSY, ROESY, HSQC, and HMBC experiments. For the 2,6-[$MeN(CH_2CH_2)_2NCH_2]_2C_6H_3$ ligand the three numbering schemes used are shown in Scheme 2 (for full numbering scheme for each compound, see Schemes S1 and S2 in ESI†).

The $^1$H NMR spectrum of **1** reveals that the coordination of nitrogen atoms to antimony in *trans* to each other as observed in solid state (*vide infra*) is retained in solution too. This behaviour is consistent with that reported previously for **2**.[23] Due to the restriction of inversion of the nitrogen atoms coordinated to the metal centre, the axial and equatorial protons of the methylene groups of the two equivalent piperazinyl rings (Scheme 2, a) give rise to four sets of multiplet resonance signals, whereas the protons of methylene groups bonded to the aromatic rings exhibit a singlet resonance signal. Heating a sample of **1** in $CDCl_3$ until 50 °C did not lead to changes in its $^1$H NMR spectrum. No changes were observed when the $^1$H and $^{13}$C NMR spectra were recorded at low temperature (213 K; see Figures S2 and S3 in ESI†).

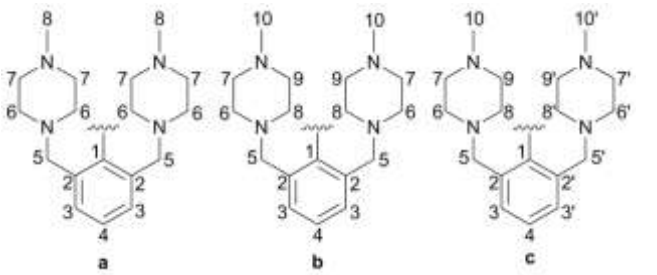


Scheme 2 Numbering scheme of the pincer ligand used in NMR assignments (**a** for compound **1**; **b** for compounds **3**-**7**, **9**-**14**; **c** for compound **8**).

In the NMR spectra of compounds **3**–**8** and **10**–**15** the methylene groups of a piperazinyl ring appear no longer equivalent two by two (Scheme 2, b), thus indicating the coordination of the nitrogen atoms in *cis* positions to the metal centre as also observed in solid state for some of the compounds (*vide infra*). As a consequence the protons of the methylene groups bonded to the aromatic ring also exhibit two AX (or AB) systems corresponding to the *pseudo*-axial (H-5a) and *pseudo*-equatorial (H-5e) positions, respectively. In all the spectra the signal corresponding to *pseudo*-axial protons is more deshielded than that corresponding to *pseudo*-equatorial protons.

In $^1$H NMR spectra of **10**, **11**, **14** and **15**, the protons of alkoxo and aryloxo ligands exhibit an AA′BB′ spin system, whereas in **12** and **13** the protons of the pinacolate ligand give rise to two singlet resonances corresponding to the methyl groups placed above and below the plane containing the $MO_2$ unit.

In compound **9** the halves of the pincer ligand with respect to the axis passing through Sb and C-4 are not equivalent (Scheme 2, **c**) due to the asymmetry of the aryloxo ligand.

In the $^1$H and $^{13}$C NMR spectra of **3** two sets of resonance signals were observed the aromatic hydrogens, for the methylene groups bonded to the aromatic ring and for the methyl groups. A DOSY experiment suggested that only dimer species are present in solution, which is consistent with the



 

oligomerization degree established in solid state (*vide infra*). Therefore, as previously described for *cyclo*-[2,6-$(Me_2NCH_2)_2C_6H_3]_2Sb_2O_2$,[4] and the related dinuclear thio species *cyclo*-$R_2Sb_2S_2$,[27-29] these two sets of resonances could correspond to the *syn* and *anti* isomers (relative orientation of the Sb–C bonds with respect to a $Sb_2O_2$ ring) present in solution. Nevertheless, using the available NMR data, a definitive assignment of the resonances to a particular isomer was not possible. Dilution experiments suggest the absence of an equilibrium between the species present in solution, the molar ratio of the isomers, based on the integrals of the aromatic protons, being ca. 1:0.8. The coalescence of the resonance signals of the two isomers was not reached by heating samples of **3** in $C_6D_5CD_3$ up to 95 °C.

Two sets of resonances for the aromatic protons were also observed in the NMR spectra of the ionic, dinuclear species **5**, suggesting that geometric isomers are present in this case too in solution. In contrast to the aliphatic region of the spectrum of **3**, the resonance signals are much broader, consistent with a dynamic process, and one cannot identify the resonances corresponding to the protonated and non-protonated pendant arms.

Unlike in the case of **3**, for the organobismuth(III) analogue **4** only one set of resonance signals was observed in the NMR spectra, consistent with the presence of only one isomer in the freshly prepared $CDCl_3$ solution. This contrasts with the presence of both *syn* and *anti* isomers (relative orientation of the Bi–C bonds with respect to a $Bi_2S_2$ ring) in $CDCl_3$ solution of related dinuclear sulphide *cyclo*-[2,6-$(^tBuOCH_2)_2C_6H_3]_2Bi_2S_2$.[29]

**X-ray crystallography**

Crystals suitable for single-crystal X-ray diffraction studies were obtained for the dichloride **1**, the oxides **3** and **4**·$4H_2O$, the ionic species **5**·$H_2O$·$C_6H_5Me$, the oxalate **8**·$H_2O$, the alkoxides **10**·$2H_2O$, **11**·$2H_2O$ and **12**, as well as the aryloxides **14** and **15**. For compound **5**·$H_2O$·$C_6H_5Me$ the reported data are those obtained at low temperature, since at room temperature a high disorder of the trifluoroacetate groups and toluene molecule was noted. The solid state molecular structures of representative compounds are depicted in Figures 1–7 (for the rest of compounds, see Figures S45, S50 and S58 in ESI†). Selected interatomic distances and angles are summarized in Tables 1–3.

The crystal of the dichloride **1** contains two independent molecules (**1a** and **1b**) in the unit cell. Their molecular parameters are very similar (Table 1) and in the subsequent discussion we will refer only to molecule **1a**. The molecular structure features a T-shaped $CSbCl_2$ core, with *trans* chlorine atoms [Cl–Sb–Cl 172.32(3)°], similar to that found in [2,6-$(Me_2NCH_2)_2C_6H_3]SbCl_2$,[16] or in the related organobismuth(III) dihalides: [2,6-$(Me_2NCH_2)_2C_6H_3]BiX_2$ (X = Cl, Br, I],[17] or [2,6-{$MeN(CH_2CH_2)_2NCH_2\}_2C_6H_3]BiX_2$ [X = Cl (**2**), Br, I].[23]

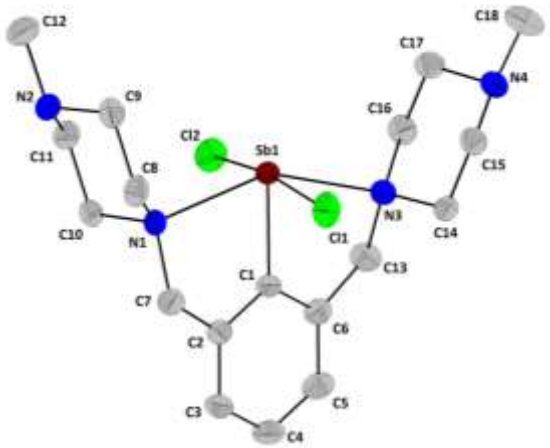


Fig. 1 Molecular structure of isomer ($pS_{N1}$,$pS_{N3}$)-**1a**. Thermal ellipsoids are drawn at the 30% probability. Hydrogen atoms are omitted for clarity.

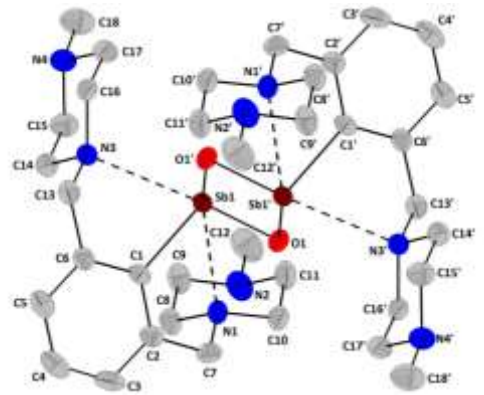


Fig. 2 Molecular structure of isomer *anti*-($pR_{N1}$,$pS_{N3}$)($pS_{N1'}$,$pR_{N3'}$)-**3**. Thermal ellipsoids are drawn at the 30% probability. Hydrogen atoms are omitted for clarity.

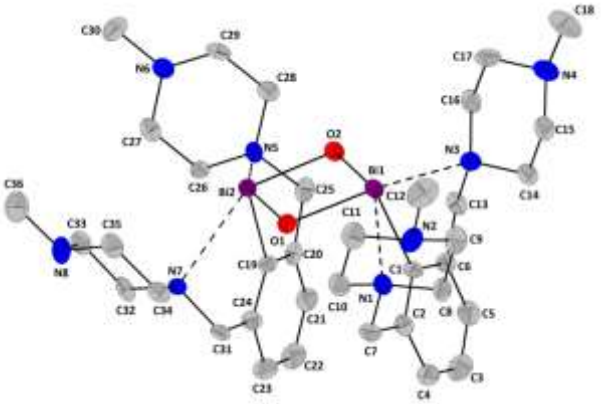


Fig. 3 Molecular structure of isomer *syn*-($pR_{N1}$,$pS_{N3}$)($pR_{N5}$,$pS_{N7}$)-**4**. Thermal ellipsoids are drawn at the 25% probability. Hydrogen atoms are omitted for clarity.

The Sb–Cl bonds are slightly asymmetric [2.5857(7) / 2.6356(7) Å] and considerably longer than the sum of covalent radii for the corresponding atoms [$\Sigma r_{cov}$(Sb,Cl) 2.40 Å],[30] consistent with the 3c-4e theory of the hypervalent bond formation. This T-shaped $CSbCl_2$ core is stabilized through

**Table 1** Selected bond distances (Å) and angles (°) for compounds **1**, **3** and **5**·$H_2O$·$C_6H_5Me$

| **1** | molecule **1a** | molecule **1b** | **3** | | **5**·$H_2O$·$C_6H_5Me$ | |
|---|---|---|---|---|---|---|
| Sb(1)–C(1) | 2.115(2) | | Sb(1)–C(1) | 2.167(6) | Sb(1)–C(1) | 2.139(6) |
| Sb(1)–Cl(1) | 2.6356(7) | | Sb(1)–O(1) | 2.012(4) | Sb(1)–O(1) | 2.207(3) |
| Sb(1)–Cl(2) | 2.5857(7) | | Sb(1)–O(1′) | 2.002(4) | Sb(1)–O(2) | 1.994(3) |
| Sb(1)–N(1) | 2.4734(19) | | Sb(1)–N(1) | 2.835(5) | Sb(1)–N(1) | 2.889(5) |
| Sb(1)–N(3) | 2.505(2) | | Sb(1)–N(3) | 2.742(5) | Sb(1)–N(3) | 2.460(4) |
| Sb(2)–C(19) | | 2.103(2) | | | Sb(2)–C(19) | 2.157(6) |
| Sb(2)–Cl(3) | | 2.6307(7) | | | Sb(2)–O(1) | 2.112(3) |
| Sb(2)–Cl(4) | | 2.5855(8) | | | Sb(2)–O(2) | 1.991(3) |
| Sb(2)–N(5) | | 2.4708(19) | | | Sb(2)–N(5) | 2.587(4) |
| Sb(2)–N(7) | | 2.475(2) | | | Sb(2)–N(7) | 2.934(4) |
| | | | | | O(1)–H(1A) | 0.84(4) |
| C(1)–Sb(1)–Cl(1) | 86.76(6) | | C(1)–Sb(1)–O(1) | 96.18(19) | C(1)–Sb(1)–O(1) | 94.76(18) |
| C(1)–Sb(1)–Cl(2) | 85.57(6) | | C(1)–Sb(1)–O(1′) | 96.92(18) | C(1)–Sb(1)–O(2) | 90.34(18) |
| C(1)–Sb(1)–N(1) | 75.18(8) | | C(1)–Sb(1)–N(1) | 67.79(19) | C(1)–Sb(1)–N(1) | 66.32(18) |
| C(1)–Sb(1)–N(3) | 74.79(7) | | C(1)–Sb(1)–N(3) | 70.0(2) | C(1)–Sb(1)–N(3) | 74.30(17) |
| Cl(1)–Sb(1)–Cl(2) | 172.32(3) | | O(1)–Sb(1)–N(3) | 149.07(16) | O(1)–Sb(1)–N(3) | 153.99(13) |
| N(1)–Sb(1)–N(3) | 149.95(6) | | O(1′)–Sb(1)–N(1) | 149.63(16) | O(2)–Sb(1)–N(1) | 137.64(14) |
| Cl(1)–Sb(1)–N(1) | 83.09(5) | | O(1)–Sb(1)–O(1′) | 79.80(16) | O(1)–Sb(1)–O(2) | 74.91(13) |
| N(1)–Sb(1)–Cl(2) | 95.23(5) | | O(1′)–Sb(1)–N(3) | 74.84(15) | O(2)–Sb(1)–N(3) | 81.52(14) |
| Cl(2)–Sb(1)–N(3) | 83.45(5) | | N(3)–Sb(1)–N(1) | 119.89(14) | N(3)–Sb(1)–N(1) | 121.25(14) |
| N(3)–Sb(1)–Cl(1) | 94.24(5) | | N(1)–Sb(1)–O(1) | 76.20(14) | N(1)–Sb(1)–O(1) | 72.61(14) |
| C(19)–Sb(2)–Cl(3) | | 83.71(6) | | | C(19)–Sb(2)–O(1) | 86.65(17) |
| C(19)–Sb(2)–Cl(4) | | 86.75(6) | | | C(19)–Sb(2)–O(2) | 103.05(17) |
| C(19)–Sb(2)–N(5) | | 75.12(8) | | | C(19)–Sb(2)–N(5) | 72.92(17) |
| C(19)–Sb(2)–N(7) | | 75.37(8) | | | C(19)–Sb(2)–N(7) | 68.02(16) |
| Cl(3)–Sb(2)–Cl(4) | | 170.45(3) | | | O(1)–Sb(2)–N(5) | 142.57(14) |
| N(5)–Sb(2)–N(7) | | 150.48(7) | | | O(2)–Sb(2)–N(7) | 149.41(13) |
| Cl(3)–Sb(2)–N(5) | | 82.54(5) | | | O(1)–Sb(2)–O(2) | 77.16(13) |
| N(5)–Sb(2)–Cl(4) | | 95.51(5) | | | O(2)–Sb(2)–N(5) | 77.43(14) |
| Cl(4)–Sb(2)–N(7) | | 83.39(5) | | | N(5)–Sb(2)–N(7) | 123.64(12) |
| N(7)–Sb(2)–Cl(3) | | 93.68(5) | | | N(7)–Sb(2)–O(1) | 73.24(13) |
| | | | Sb(1)–O(1)–Sb(1′) | 100.20(18) | Sb(1)–O(1)–Sb(2) | 98.05(14) |
| | | | | | Sb(1)–O(2)–Sb(2) | 109.84(16) |
| | | | | | Sb(1)–O(1)–H(1A) | 110(3) |
| | | | | | Sb(2)–O(1)–H(1A) | 110(3) |

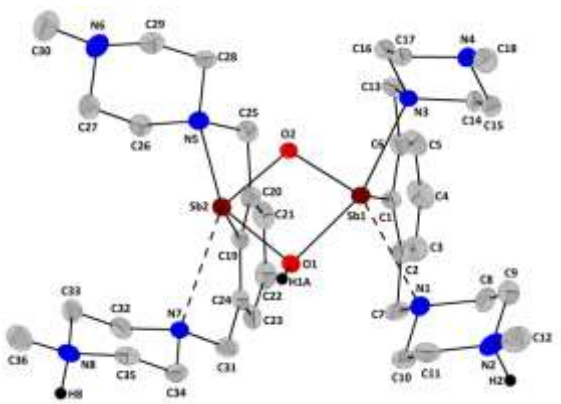

Fig. 4 Structure of the cation in isomer *syn-meso*-($A_{Sb1}$,$pR_{N1}$,$pS_{N3}$)($C_{Sb2}$,$pS_{N7}$,$pR_{N5}$)-**5**. Thermal ellipsoids are drawn at the 25% probability. For clarity, only the hydrogen atom of the hydroxy group is shown.

intramolecular N→Sb interactions placed *trans* to each other [N–Sb–N 149.95(6)°], thus resulting in an overall distorted square pyramidal (*N*,*C*,*N*)$SbCl_2$ core. The interatomic Sb–N distances are of the same magnitude in **1a** [2.4734(19) / 2.505(2) Å] compared to those observed in [2,6-$(Me_2NCH_2)_2C_6H_3$]$SbCl_2$ [2.422(8) / 2.491(9) Å].[16] It should be noted here that the difluoride [2,6-$(Me_2NCH_2)_2C_6H_3$]$SbF_2$ exhibits a pyramidal $CSbF_2$ core, with longer additional intramolecular N→Sb interactions [2.579(5) / 2.598(7) Å] *cis* to each other and placed *trans* to the fluorine atoms.[31,32]

The non-planarity of the five-membered $MC_3N$ chelate ring formed as result of an intramolecular N→M interaction induces planar chirality [with the aromatic ring and the nitrogen atom as chiral plane and pilot atom, respectively],[33] a pattern common for many related compounds.[1,34] Indeed, the crystal of **1** contains 1:1 mixtures of ($pS_{N1}$,$pS_{N3}$)- and ($pR_{N1}$,$pR_{N3}$)-**1a** and ($pS_{N5}$,$pS_{N7}$)- and ($pR_{N5}$,$pR_{N7}$)-**1b** isomers (with respect to the two chelate rings in a molecular unit), respectively, as reported previously for the bismuth analogue **2**.[23]

The molecules of the compounds **3**–**5**, **8**, **10**–**12**, **14** and **15**, regardless the number of metal atoms per molecular unit, their neutral or ionic nature and the nature of the oxo ligand, exhibit a common feature, *i.e.* an overall distorted square pyramidal (*N*,*C*,*N*)$MO_2$ core, with *cis* intramolecular N→M interactions placed in *trans* to M–O bonds. The N–M–N angles range between 119.89(14)° and 126.45(10)° for the antimony species, and between 117.1(2) and 124.83(15)° for the bismuth

compounds **4**, **11** and **15**. The most acute N–M–N angles are observed for the cyclic oxides **3** [N–Sb–N 119.89(14)°] and **4** [N–Bi–N 117.1(2) / 119.5(2)°]. For comparison, in the related *cyclo*-[2,6-$(Me_2NCH_2)_2C_6H_3]_2Sb_2O_2$ the N–Sb–N angle is 121.84(10)°.[4]

An important difference between the two cyclic oxides is concerned to the relative orientation of the M–C bonds with respect to a $M_2O_2$ ring. Thus, while the crystal of the antimony species **3** contained the *anti* isomer, for the bismuth analogue **4** the *syn* isomer was found. The crystals of the related *cyclo*-[2,6-$(Me_2NCH_2)_2C_6H_3]_2Sb_2O_2$,[4] as well as those of the other few dinuclear oxides with bulky organic groups, *i.e. cyclo*-[2,4,6-$\{(Me_3Si)_2CH\}_3C_6H_2]_2M_2O_2$ (M = Sb,[35] Bi[36]), always contained the *anti* isomer. It should be noted that a trinuclear *cyclo*-[2-$(Me_2NCH_2)C_6H_4]_3Sb_3O_3$, containing a ligand with only one pendant arm and exhibiting a *syn-anti* orientation of the substituents,[27] or a tetrameric $[(Me_3Si)_2CH]_4Sb_4O_4$ species,[37] were also described.

Some differences can be also observed in the molecular parameters of the cyclic oxides **3** and **4**. Within the planar $M_2O_2$ ring the M–O bonds are of the same length within experimental errors: Sb–O 2.002(4) / 2.012(4) Å in **3** [cf. Sb–O 2.000(3) / 2.018(3) Å for *cyclo*-[2,6-$(Me_2NCH_2)_2C_6H_3]_2Sb_2O_2$][4] and Bi–O 2.133(7)–2.146(7) Å in **4** [cf. Bi–O 2.070(8) / 2.103(12) Å for *cyclo*-[2,4,6-$\{(Me_3Si)_2CH\}_3C_6H_2]_2Bi_2O_2$].[36] By contrast, the M–N interatomic distances are slightly asymmetric in **3** [2.742(5) / 2.835(5) Å] (an even higher asymmetry, *i.e.* Sb–N 2.641(6)/2.800(3) Å, was reported for *cyclo*-[2,6-$(Me_2NCH_2)_2C_6H_3]_2Sb_2O_2$][4]), but symmetrical in **4** [range 2.796(8)–2.836(8) Å]. In both cases they are considerably longer than in the diclorides **1a** [Sb–N 2.4734(19) / 2.505(2) Å] and **2** [Bi–N 2.563(4) / 2.583(5) Å] used as starting materials, but shorter than the sum of van der Waals radii for the corresponding atoms [$\Sigma r_{vdW}$(Sb,N) 3.74 Å; $\Sigma r_{vdW}$(Bi,N) 3.94 Å].[30]

In contrast to the oxide **3**, the cyclic cation of the species **5** exhibited a *syn* orientation of the Sb–C bonds with respect to the $Sb_2O_2$ ring. The presence of different oxo and hydroxo bridges, respectively, between the Sb atoms is reflected in the degree of asymmetry of the central, planar $Sb_2O_2$ ring: the angle Sb–O(H)–Sb is more acute [98.05(14)°] than the Sb–O–Sb [109.84(16)°], while the Sb–O(H) bond lengths are longer [2.207(3) / 2.112(3) Å] than the Sb–O bond lengths [1.994(3) / 1.991(3) Å]. Consequently, there is a clear difference in the lengths of the Sb–N interactions, *i.e.* shorter Sb–N interactions [2.460(4) / 2.587(4) Å] are *trans* to the longer Sb–O(H) bonds and significantly longer Sb–N interactions [2.889(5) / 2.934(4) Å] are placed *trans* to the shorter Sb–O bonds.

The planar chirality due to folded $MC_3N$ chelate rings is also present in the molecules of the dinuclear compounds **3**–**5**. However, the molecule of **3** has an inversion centre and therefore the chirality of the whole molecule is lost even if some asymmetry in the intramolecular N→Sb interactions was noted and the crystal of this oxide contains only the isomer *anti*-($pR_{N1}$,$pS_{N3}$)($pS_{N1'}$,$pR_{N3'}$)-**3** (Figure 2). The same absence of chirality is noted for the whole molecule of the oxide **4**

**Table 2** Selected bond distances (Å) and angles (°) for compounds **8**·$H_2O$, **10**·$2H_2O$, **12** and **14**

| | **8**·$H_2O$ | **10**·$2H_2O$ | **12** | **14** |
|---|---|---|---|---|
| Sb(1)–C(1) | 2.142(5) | 2.192(11) | 2.155(5) | 2.153(4) |
| Sb(1)–O(1) | 2.116(3) | 2.020(8) | 2.011(3) | 2.056(3) |
| Sb(1)–O(2) | 2.122(3) | 2.053(8) | 2.006(4) | 2.075(3) |
| Sb(1)–N(1) | 2.594(3) | 2.705(9) | 2.801(5) | 2.634(3) |
| Sb(1)–N(3) | 2.606(4) | 2.737(9) | 2.704(5) | 2.697(3) |
| C(19)–O(1) | 1.304(4) | 1.405(17) | 1.428(5) | 1.345(5) |
| C(20)–O(2) | 1.302(5) | 1.414(17) | 1.428(6) | 1.359(5) |
| C(19)–C(20) | 1.546(6) | 1.46(2) | 1.543(7) | 1.393(5) |
| C(19)–O(3) | 1.215(5) | | | |
| C(20)–O(4) | 1.206(5) | | | |
| C(1)–Sb(1)–O(1) | 92.66(14) | 95.5(4) | 96.63(16) | 93.82(13) |
| C(1)–Sb(1)–O(2) | 92.75(13) | 95.4(3) | 96.45(17) | 94.74(13) |
| C(1)–Sb(1)–N(1) | 72.15(14) | 70.3(3) | 69.04(17) | 71.59(11) |
| C(1)–Sb(1)–N(3) | 71.92(15) | 70.9(3) | 70.77(17) | 70.71(11) |
| O(1)–Sb(1)–N(3) | 145.32(10) | 151.4(3) | 148.54(13) | 146.88(10) |
| O(2)–Sb(1)–N(1) | 145.42(11) | 149.2(3) | 148.91(12) | 147.48(10) |
| O(1)–Sb(1)–O(2) | 76.09(11) | 81.9(3) | 81.09(13) | 78.96(11) |
| O(2)–Sb(1)–N(3) | 73.94(10) | 74.7(3) | 72.23(13) | 73.60(10) |
| N(3)–Sb(1)–N(1) | 126.45(10) | 122.2(3) | 123.75(13) | 125.18(10) |
| N(1)–Sb(1)–O(1) | 73.84(10) | 72.8(3) | 73.86(13) | 72.90(11) |
| Sb(1)–O(1)–C(19) | 118.0(3) | 111.9(8) | 113.7(3) | 112.6(2) |
| Sb(1)–O(2)–C(20) | 117.6(3) | 109.1(7) | 111.7(3) | 111.7(2) |
| O(1)–C(19)–C(20) | 114.0(4) | 114.3(12) | 106.5(3) | 117.2(3) |
| O(1)–C(19)–C(24) | | | | 122.6(3) |
| C(20)–C(19)–C(24) | | | | 120.2(4) |
| O(2)–C(20)–C(19) | 114.3(3) | 111.1(11) | 106.8(4) | 117.1(4) |
| O(2)–C(20)–C(21) | | | | 123.4(3) |
| C(19)–C(20)–C(21) | | | | 119.5(4) |
| O(3)–C(19)–C(20) | 121.6(3) | | | |
| O(1)–C(19)–O(3) | 124.4(4) | | | |
| O(4)–C(20)–C(19) | 121.4(4) | | | |
| O(2)–C(20)–O(4) | 124.3(4) | | | |

(within experimental errors, a plane of symmetry, passing through the antimony atoms and the carbon atoms attached to them, is present), the crystal containing only the isomer *syn*-($pR_{N1}$,$pS_{N3}$)($pR_{N5}$,$pS_{N7}$)-**4** (Figure 3). If the differences in the antimony-nitrogen interatomic distances in the solid state are not considered, the ionic species **5** appears to contain the *syn-meso*-($A_{Sb1}$,$pR_{N1}$,$pS_{N3}$)($C_{Sb2}$,$pS_{N7}$,$pR_{N5}$)-**5** diastereomer of the cation (Figure 4) [the chirality at the antimony atom in the square pyramidal (*N*,*C*,*N*)SbO(OH) core can be described in term of $C_{Sb}$ and $A_{Sb}$ isomers].[38] However, in the cation the equivalent Sb–N bonds and N→Sb interactions for the two metal centers are different [2.460(4) / 2.587(4) Å and 2.889(5) / 2.934(4) Å, respectively] within experimental errors and if this is taken into account one can distinguish pairs of enantiomers in the crystal of **5** (see Figure S18 in ESI†).

The mononuclear organoantimony(III) species **8**, **10**, **12** and **14** exhibit Sb–O distances [2.006(4)–2.122(3) Å] in the normal range for covalent bond lengths, an increase being observed in the order 1,3,2-dioxastibolanes **10** and **12** < 1,3,2-dioxastibole **14** < oxalate **8**. Consequently, the shorter Sb–N distances are observed in **7** and the longer in the 1,3,2-dioxastibolanes. For the related organobismuth(III) compounds **11** and **15**, while the Bi–O distances are of the same magnitude as found in the oxide **4**, the interatomic distances corresponding to the intramolecular N→Bi interactions follow the same pattern as for the antimony

**Table 3** Selected bond distances (Å) and angles (°) for compounds **4**·4$H_2O$, **11**·2$H_2O$ and **15**

| | **4**·4$H_2O$ | **11**·2$H_2O$ | **15** |
|---|---|---|---|
| Bi(1)–C(1) | 2.267(11) | 2.235(5) | 2.243(5) |
| Bi(1)–O(1) | 2.133(7) | 2.137(4) | 2.169(4) |
| Bi(1)–O(2) | 2.146(7) | 2.167(3) | 2.189(4) |
| Bi(1)–N(1) | 2.816(8) | 2.724(5) | 2.672(5) |
| Bi(1)–N(3) | 2.813(8) | 2.743(4) | 2.729(5) |
| Bi(2)–C(19) | 2.254(10) | | |
| Bi(2)–O(1) | 2.143(7) | | |
| Bi(2)–O(2) | 2.137(7) | | |
| Bi(2)–N(5) | 2.836(8) | | |
| Bi(2)–N(7) | 2.796(8) | | |
| C(1)–Bi(1)–O(1) | 94.8(3) | 93.95(16) | 93.18(18) |
| C(1)–Bi(1)–O(2) | 96.6(3) | 94.27(15) | 94.16(18) |
| C(1)–Bi(1)–N(1) | 68.6(3) | 69.26(16) | 70.40(17) |
| C(1)–Bi(1)–N(3) | 67.2(3) | 69.65(15) | 69.67(16) |
| O(1)–Bi(1)–N(3) | 146.5(3) | 147.96(13) | 144.69(16) |
| O(2)–Bi(1)–N(1) | 148.3(3) | 146.07(14) | 144.65(13) |
| O(1)–Bi(1)–O(2) | 78.8(3) | 78.55(13) | 76.62(14) |
| O(2)–Bi(1)–N(3) | 75.8(2) | 75.61(14) | 74.26(15) |
| N(3)–Bi(1)–N(1) | 119.5(2) | 121.63(12) | 124.83(15) |
| N(1)–Bi(1)–O(1) | 75.0(3) | 73.48(12) | 72.88(14) |
| C(19)–Bi(2)–O(1) | 97.5(3) | | |
| C(19)–Bi(2)–O(2) | 94.4(3) | | |
| C(19)–Bi(2)–N(5) | 67.7(3) | | |
| C(19)–Bi(2)–N(7) | 68.3(3) | | |
| O(1)–Bi(2)–N(5) | 151.2(2) | | |
| O(2)–Bi(2)–N(7) | 147.0(3) | | |
| O(1)–Bi(2)–O(2) | 78.7(3) | | |
| O(2)–Bi(2)–N(5) | 78.0(2) | | |
| N(5)–Bi(2)–N(7) | 117.1(2) | | |
| N(7)–Bi(2)–O(1) | 76.2(3) | | |
| Bi(1)–O(1)–Bi(2) | 101.4(3) | | |
| Bi(1)–O(2)–Bi(2) | 101.1(3) | | |
| Bi(1)–O(1)–C(19) | | 111.7(3) | 112.0(3) |
| Bi(1)–O(2)–C(20) | | 108.6(3) | 111.6(3) |
| O(1)–C(19)–C(20) | | 114.6(5) | 118.3(5) |
| O(1)–C(19)–C(24) | | | 122.1(5) |
| C(20)–C(19)–C(24) | | | 119.6(6) |
| O(2)–C(20)–C(19) | | 114.2(6) | 118.5(5) |
| O(2)–C(20)–C(21) | | | 122.6(5) |
| C(19)–C(20)–C(21) | | | 118.8(5) |

analogues, *i.e.* they are slightly shorter for the 1,3,2-dioxabismole **15** than for the 1,3,2-dioxabismolane **11**.

The $MO_2C_2$ ring in oxalate **8** is planar, while in the catecholates **14** and **15** the metal atoms are slightly displaced from the best plane defined by the rest of the atoms of the chelate ring (the dihedral angle between $MO_2$ and $O_2C_2$ planes is 14.0° in **14** and 14.8° in **15**, respectively). By contrast, in the alkoxides **10**–**12** the $MO_2C_2$ rings are not planar, but one of the carbon atoms is pushed out of the best plane defined by the rest of the atoms (the dihedral angle between best $MO_2C$ and $OC_2$ planes is 34.3° in **10**, 33.8° in **11** and 39.3° in **12**, respectively). The non-planarity of the chelate ring induces chirality and indeed their crystals contain 1:1 mixture of ($\delta$-$pS_N$,$pR_N$) and ($\lambda$-$pR_N$,$pS_N$) isomers.

In addition to intramolecular Cl···H and O···H contacts which are present in the molecular units of all compounds (for details, see Figures S4, S10, S12, S19, S33, S42, S47, S52, S59 and S64 in ESI†), supramolecular associations are observed in all structures, except the oxide **3**. In the crystal of the dichloride

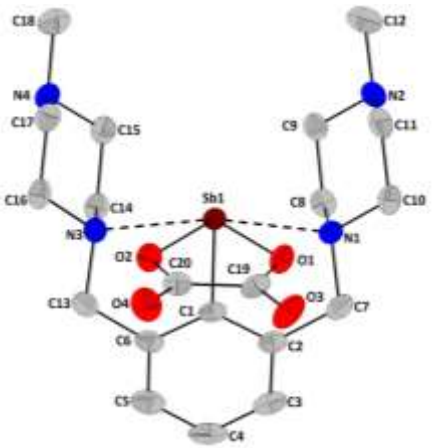


Fig. 5 Molecular structure of the isomer ($pR_{N1}$,$pS_{N3}$)-**8**. Thermal ellipsoids are drawn at the 30% probability. Hydrogen atoms are omitted for clarity.

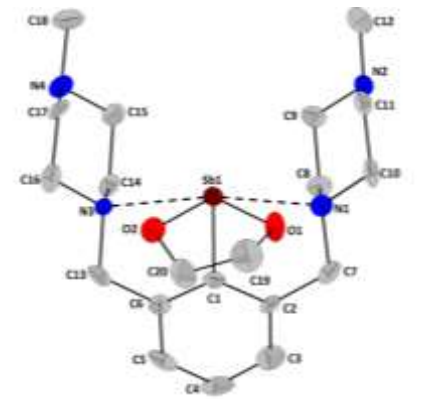


Fig. 6 Molecular structure of the isomer ($\lambda$-$pR_{N1}$,$pS_{N3}$)-**10**. Thermal ellipsoids are drawn at the 30% probability. Hydrogen atoms are omitted for clarity.

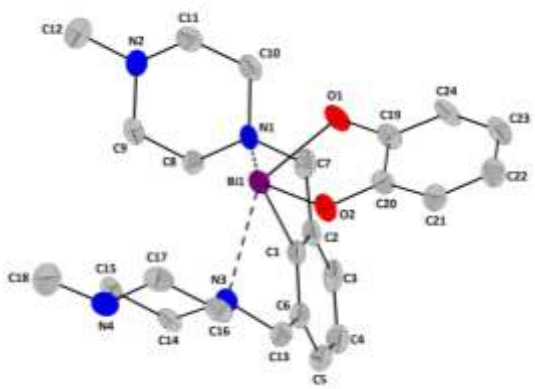


Fig. 7 Molecular structure of the isomer ($pR_{N1}$,$pS_{N3}$)-**15**. Thermal ellipsoids are drawn at the 25% probability. Hydrogen atoms are omitted for clarity.

**1** the molecules are connected through Cl···H contacts into layers without further contacts between parallel layers (see Figures S5 and S6 in ESI†). When water of crystallization is present, polymeric chains are formed based on N···$H_{water}$ (**8**·$H_2O$ – Figure S34; **11**·2$H_2O$ – Figure S48 in ESI†) or N···$H_{water}$ / O···$H_{water}$ contacts (**10**·2$H_2O$ – Figures S43 and S44

in ESI†). For the ionic species $\mathbf{5}\cdot H_2O\cdot C_6H_5Me$ a more complicated 3D architecture is established through O···H, C–H···π ($Ar_{centroid}$) and C–F···π ($Ar_{centroid}$) contacts (for details, see Figures S20 and S21 in ESI†).

1D-Chains of the type $(syn\text{-}R_2Bi_2O_2\cdot H_2O)_n$ are formed by dinuclear oxide units connected through hydrogen bonds [N(6)···H(5Ba)$_{water}$ 2.12, N(8)···H(5A)$_{water}$ 2.13 Å] involving water molecules in the crystal of $\mathbf{4}\cdot 4H_2O$. Water hexamer units with a [tetramer+2] structure are fixed between two such 1D-chains resulting in a supramolecular polymeric arrangement (see Figures S13 and S14 in ESI†). To the best of our knowledge this is the first reported example of such structural motif, theoretically predicted to have binding energy much larger than other water hexamer clusters[39] which were experimentally encountered.[40,41] This particular arrangement in the crystal of $\mathbf{4}\cdot 4H_2O$ is stabilized by additional hydrogen bonds between the [tetramer+2] structure and oxygen atoms of the organobismuth(III) compound (Figure 8).

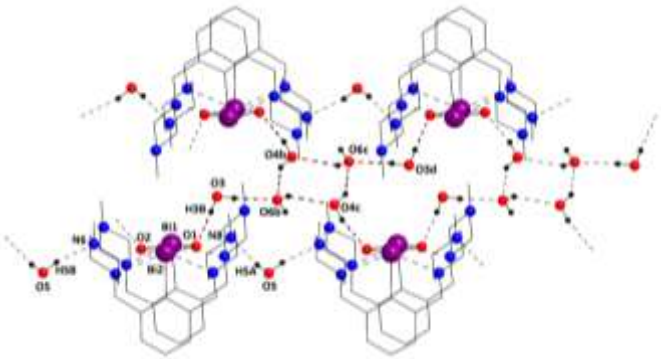

Fig. 8 Supramolecular architecture in the crystal of $\mathbf{4}\cdot 4H_2O$ showing the hexamer water cluster with [tetramer+2] motif fixed between two 1D-chains of $(syn\text{-}R_2Bi_2O_2\cdot H_2O)_n$.

In the crystals of compounds **12**, **14** and **15** there are intermolecular C–H···π ($Ar_{centroid}$) distances consistent with π interactions (*i.e.* H···$Ar_{centroid}$ contacts shorter than 3.1 Å, with an angle γ between the normal to the aromatic ring and the line defined by the H atom and $Ph_{centroid}$ smaller than 30°).[42] These interactions lead to dimer (for **12** – Figure S53 in ESI†), chain polymer (for **15** – Figure S65 in ESI†) and honeycomb layer (for **14** – Figures S60 and S61 in ESI†) associations, with no further contacts between these supramolecular entities.

### Theoretical studies

The intramolecular coordination of the pendant arms to the metal centre in **1** brings a stabilization of the square pyramidal geometry at antimony of 35.59 kcal·mol$^{-1}$. In the calculated structure with only one arm coordinated to the metal and with the chlorine atoms in position *trans* to each other, the stabilization amounts 22.09 kcal·mol$^{-1}$ (see Figures S66-S68 in ESI†). These values compare well with those reported for analogous bismuth species with the pincer ligand 2,6-$(Me_2NCH_2)_2C_6H_3$.[17]

In order to probe the stabilization energy brought by the coordination of the pendant arms to pnicogen in positions *cis* to each other, calculations were performed on **10** and **11** (see Figures S86-S91 in ESI†). In this case the structures with one arm coordinated to the metal centre have energies larger than those of the structures found in the crystal with 12.50 and 14.11 kcal·mol$^{-1}$, respectively. If both arms are uncoordinated from the metal centre the energies are with 29.19 and 30.97 kcal·mol$^{-1}$ larger, respectively. The smaller values found for the stabilization energies when the two pendant arms are coordinated in position *cis* are consistent to the increase in the steric repulsions between piperanzyl groups. At the same time, the small value of energy required for the uncoordination of one arm is also consistent to the dynamic behaviour observed in solution by NMR spectroscopy for both **10** and **11**.

Theoretical calculations revealed that in gas phase for oxides **3** and **4** the *syn* isomers are favoured with respect to the *anti* isomers with 2.29 kcal·mol$^{-1}$ and 3.30 kcal·mol$^{-1}$, respectively. This is consistent with the *syn* structure determined for the bismuth species **4**, but contrast to the *anti* structure determined for the antimony analogue **3**. The energy calculated for the minima structures of *syn* isomers of **3** and **4** is smaller than the energy of two RM=O (M = Sb, Bi) monomers with 78.78 and 82.48 kcal·mol$^{-1}$, respectively. Nevertheless, these values, at least for **3**, are consistent to the solution behaviour of the compound, where both *syn* and *anti* isomers were observed.

The different ligand arrangement with respect to the $Sb_2O_2$ core in the cation of **5** *vs.* the starting material **3** raised the question which isomer for this compound is favoured in the gas phase. In this case, the results are consistent to the crystal structure, the energy of *syn* isomer of the model cation $[(RSb)_2(\mu\text{-}O)(\mu\text{-}OH)]^+$ being slightly smaller (with 4.88 kcal·mol$^{-1}$) than that of the *anti* isomer. Nevertheless this energy difference is still comparable to the values obtained for the isomers of the oxides. It was interesting to probe whether it is favourable to have the protons bonded to nitrogen groups on the same or on different pincer ligands. In the gas phase, the cation of **5**, with the protons bonded to different pincer ligands, similar to the arrangement found in crystal, has an energy with 11.57 kcal·mol$^{-1}$ smaller than the energy corresponding to the structure where the protons are bonded to the same pincer, presumably as a consequence of a preference to have a more uniformly distribution of charge through the molecule.

For the carbonate **6**, in absence of relevant crystallographic data, at least three structures that correspond to the experimental data, are possible. In the first model $CO_3$ can act as a bidentate ligand coordinated to antimony in a terminal fashion, whereas in the other models it can act as a bridging bidentate ligand between two metal centres (see Figures S79-S81 in ESI†). For the dimer with two bridging $CO_3$ groups, several isomers are possible due to the different relative orientations of the carbonate and of the pincer ligands. The energies of two of the possible structures (see Figures S80 and S81 in ESI†) of *syn* and *anti* isomers of the dimeric carbonate are with 22.89 and 20.59 kcal·mol$^{-1}$, respectively, lower than the energy corresponding to two units of carbonate bonded in a terminal fashion. The energy of these two structures of the

carbonate is also smaller than the energy of the corresponding isomer of **3** and two $CO_2$ molecules with 12.12 and 12.10 kcal·mol$^{-1}$, respectively. Nevertheless the theoretically calculated Gibbs free energies (15.72 and 15.18 kcal·mol$^{-1}$) for the reaction of the *syn* and *anti* isomers of **3** and two molecules of $CO_2$ suggests that the process should not be spontaneous. With respect to the formation of dimers from a mononuclear species with a bidentate $CO_3$ group, the Gibbs free energies (–5.51 and –2.98 kcal·mol$^{-1}$), although small and in the range of the errors found for the DFT method used,[43] suggest that the process should be spontaneous.

For compound **6** the possible structure of an oxo-carbonate $(RSb)_2(\mu\text{-}O)(\mu\text{-}CO_3)$ (see Figures S82 and S83 in ESI†), formed by the reaction of **3** with only one molecule of $CO_2$, was also considered. For this compound, *syn* and *anti* isomers can also exist, due to two possible orientations of the pincer ligands with respect to the plane containing the $Sb_2O$ core. In this case the energy of the *syn* and *anti* isomers of the oxo-carbonate is 8.66 and 10.33 kcal·mol$^{-1}$, respectively, smaller than the energy of the corresponding isomers of oxide **3** and one molecule of $CO_2$ and in the range of the values found for the dimers (*vide supra*). The calculated Gibbs free energies for these reactions (5.32 and 3.27 kcal·mol$^{-1}$) suggest the formation of the oxo-carbonate is a non-spontaneous process. Nevertheless the small values of the Gibbs free energy, at least in the framework of the used method, suggest that the formation of the oxo-carbonate is a more likely process than the formation of dimers.

The formation of the organoantimony(III) compounds with chelating ligands was also investigated using DFT calculations. For the neutral compounds **8**, **10**, **12** and **14** and the cation of **9** the Gibbs free energy between the products and starting materials reveal that formation of the chelates in the gas phase from both the *anti* and the *syn* isomer of **3** and the corresponding 1,2-dihydroxy derivatives is a spontaneous process. The calculated Gibbs free energies change upon the formation of the chelates from the *syn* isomer of **3** are –28.50 for **8**, –39.59 for the cation of **9**, –8.94 for **10**, –12.53 for **12**, and –21.45 kcal·mol$^{-1}$ for **14**. All the energies corresponding to the formation of the chelates from the *anti* isomer are with about 3 kcal·mol$^{-1}$ larger. These Gibbs free energy values are consistent with our experimental results for **8**-**10**, **12** and **14** where the chelates were obtained by the reactions of the mixture of isomers of **3** with the 1,2-dihydroxy derivatives. The calculated Gibbs free energies (−0.02, –20.23, and –26.25 kcal·mol$^{-1}$) for the formation of the bismuth chelates **11**, **13**, and **15**, from the *syn* isomer of **4** and the corresponding 1,2-dihydroxy derivatives also indicate a spontaneous process.

## Experimental

### General measurements and analysis instrumentation

Multinuclear NMR spectra ($^1$H, $^{13}$C, $^{19}$F) were recorded at room temperature on Bruker Avance 300, Bruker Avance III 400 or Bruker Avance III 600 instruments. Low-temperature NMR experiments were performed on the Bruker Avance 300 apparatus. The $^1$H chemical shifts are reported in $\delta$ units (ppm) relative to the residual peak of the deuterated solvent ($CHCl_3$, 7.26 ppm; HOD, 4.79 ppm). The $^{13}$C chemical shifts are reported in $\delta$ units (ppm) relative to the peak of the deuterated solvent ($CDCl_3$, 77.16 ppm).[44] $^1$H and $^{13}$C resonances were assigned using 2D NMR experiments (COSY, ROESY, HSQC, HMBC). DOSY NMR experiments for **3** were carried out on Bruker Avance III 400 spectrometer using PABBO broad band probe with pulsed field gradient. For the diffusion experiment 2D stimulated echo experiment using bipolar gradients was employed. The data were recorded at 296 K using a spectral width of 4000 Hz, 90° pulse width of 9.75 μs, a diffusion delay time of 0.05 s, and a diffusion gradient of 0.0016 s. The NMR spectra were processed using the *MestReC* and *MestReNova* software.[45] HRMS APCI(+) and ESI(+) spectra were recorded on a Thermo Scientific Orbitrap XL spectrometer. Data analysis and calculations of the theoretical isotopic patterns were carried out with the Xcalibur software package.[46] Infrared spectra were recorded in the range 4000–250 cm$^{-1}$ on a Bruker Vector 22 spectrometer. Thermogravimetric data were obtained from TA instruments SDT-Q600 analyzer.

### Crystal structure determination

Slow diffusion of petroleum ether into a $CH_2Cl_2$ solution afforded the isolation of single crystals of **1** suitable for X-ray diffraction. Slow evaporation of solutions gave single crystals of **5**·$H_2O$·$C_6H_5Me$ (from $CH_2Cl_2$:$C_6H_5Me$, 1:3 v/v), **3** and **10**·$2H_2O$ (from petroleum ether), **8**·$H_2O$ (from $CH_2Cl_2$), **11**·$2H_2O$ and **12** (from $Et_2O$), **14** and **15** (from $C_6H_5Me$). Single crystals of **4**·$4H_2O$ were obtained by slowly cooling to room temperature a hot toluene solution. The details of the crystal structure determination and refinement are given in Tables S1 – S3 (see ESI†). Crystallographic data were collected on Stoe-IPDS II (**1**) and on Bruker SMART APEX diffractometers (**3**-**5**, **8**, **10**-**12**, **14**, **15**) using graphite-monochromated Mo-Kα radiation ($\lambda$ = 0.71073 Å). The structures were solved using SIR-92,[47] or SHELXS-97,[48] and refined, with anisotropic thermal parameters for all non-hydrogen atoms, using SHELXL-2013 or SHELXL-2014/6.[49] The structures of **8**, **14** and **15** contained disordered solvents molecules which were removed using SQUEEZE procedure as implemented in PLATON.[50] The carbon and nitrogen-bonded hydrogen atoms were placed in geometrically idealized positions and refined using a riding model, whereas hydrogen atoms bonded to oxygen were restrained at H–O distance of 0.84 Å. The H···H distance in the water molecules was restrained at 1.34 Å. The isotropic displacement parameters for the hydrogen atoms were set with respect to those of the atom to which they are directly attached. The drawings were created with the Diamond program.[51] CCDC reference numbers: 1041683 (**1**), 1041684 (**3**), 1041685 (**4**·$4H_2O$), 1041686 (**5**·$H_2O$·$C_6H_5Me$), 1041687 (**8**·$H_2O$), 1041688 (**10**·$2H_2O$), 1041689 (**11**·$2H_2O$), 1041690 (**12**), 1041691 (**14**) and 1041692 (**15**).

### Computational details

Theoretical calculations were carried out using ORCA 3.0.2 software package.[52] The BP86 functional was used in conjunction with RI approximation.[53] The relativistic effects via ZORA approximation and the dispersion correction with Becke-Johnson damping were used for all calculations.[54-58] The basis sets used were def2-SVP-ZORA for H and C and def2-TZVP-ZORA for the rest of the atoms.[59,60] Very tight criteria for the SCF, tight criteria for optimization and an integration grid of **5** were employed in all the calculations. The geometries were optimized without any constraints and the structural local minima were confirmed by the absence of the imaginary frequencies. The Gibbs free energies were obtained from the frequency calculations.

**Materials and procedures**

All manipulations which involved $^{n}$BuLi were carried out under an inert atmosphere of argon using Schlenk techniques. Hexane, diethyl ether and toluene were freshly distilled prior to use, under argon atmosphere, from sodium as drying agent. All the other solvents were used as received. The $SbCl_3$ and $BiCl_3$ was freshly sublimed prior to use. Starting materials such as $^{n}$BuLi, $HOCH_2CH_2OH$, $HOCMe_2CMe_2OH$, $C_6H_4(OH)_2$-1,2, $C_6H_3(OH)_2$-1,2-$(CH_2)_2NH_2$-3·HCl, $H_2C_2O_4·2H_2O$ and $CF_3COOH$ were purchased from commercial suppliers and were used as received. The compounds 1,3-$[MeN(CH_2CH_2)_2NCH_2]_2C_6H_4$ and [2,6-$\{MeN(CH_2CH_2)_2NCH_2\}_2C_6H_3$]$BiCl_2$ (**2**) were prepared according to the literature procedure.[23]

**Synthesis of [2,6-$\{MeN(CH_2CH_2)_2NCH_2\}_2C_6H_3$]$SbCl_2$ (1).** To a solution of 1,3-$[MeN(CH_2CH_2)_2NCH_2]_2C_6H_4$ (8.34 g, 27.57 mmol) in hexane (100 mL) was added $^{n}$BuLi (18.75 mL, 1,6 M, in hexane solution) and the reaction mixture was refluxed for 3 h. The colour of the solution turned orange and a yellow solid deposited. The supernatant was removed *via* syringe and the precipitate was dried at reduced pressure. A diethyl ether suspension of the organolithium derivative thus obtained was cooled to −78 °C and then a solution of $SbCl_3$ (3.42 g, 15 mmol) in $Et_2O$ (100 mL) was added. The resulting reaction mixture was allowed to slowly reach room temperature overnight and then filtered through a glass frit. The resulting solid was washed with $Et_2O$ (2x30 mL), dried and then extracted in a Soxhlet apparatus with toluene (100 mL). Removal of the solvent *in vacuo* from the clear solution gave yellow solid which, after being washed with cold acetone (2x10 mL) afforded **1** as colourless crystalline powder (2.3 g, 31%), m.p. 235-240 °C (decomposes without melting). **$^1$H NMR** (400 MHz, $CDCl_3$, 295 K): $\delta$ 2.34 (s, 6H, H-8), 2.62 (dd, $^2J_{H\text{-}7a,H\text{-}7e} \approx {}^3J_{H\text{-}6a,H\text{-}7a}$ = 10.9 Hz, 4H, H-7a), 2.78 (dd, $^2J_{H\text{-}6a,H\text{-}6e} \approx {}^3J_{H\text{-}6a,H\text{-}7a}$ = 11.8 Hz, 4H, H-6a), 2.85 (d, $^2J_{H\text{-}7a,H\text{-}7e}$ = 12.6 Hz, 4H, H-7e), 3.76 (d, $^2J_{H\text{-}6a,H\text{-}6e}$ = 11.7 Hz, 4H, H-6e), 4.17 (s, 4H, H-5), $AB_2$ spin system with B at $\delta$ 7.18 ppm (d, $^3J_{H\text{-}3,H\text{-}4}$ = 7.5 Hz, 2H, H-3) and A at $\delta$ 7.32 ppm (t, $^3J_{H\text{-}3,H\text{-}4}$ = 7.5 Hz, 1H, H-4). **$^{13}$C{$^1$H} NMR** (101 MHz, $CDCl_3$, 295 K): $\delta$ 45.73 (C-8), 54.65 (C-6), 55.19 (br, C-7), 64.51 (br, C-5), 125.54 (C-3), 130.40 (C-4), 141.90 (C-2), 152.25 (C-1). **MS** (ESI+, MeOH): *m/z* (%) 457.11 (100) $[M-Cl-H]^+$, 421.14 (22) $[M-2Cl]^+$. HRMS (ESI+): Calc. for $[C_{18}H_{29}N_4ClSb]^+$: 457.11134. Found: 457.11234.

**Synthesis of *cyclo*-[2,6-$\{MeN(CH_2CH_2)_2NCH_2\}_2C_6H_3]_2Sb_2O_2$ (3).** A solution of KOH (0.93 g, 16.57 mmol) in ethanol (50 mL) was added over a solution of **1** (0.8 g, 1.62 mmol) in ethanol (50 mL). The reaction mixture was stirred for 24 h at room temperature, then the solvent was removed *in vacuo*. The remaining solid was dissolved in $CH_2Cl_2$, the solution was dried over anh. $Na_2SO_4$, then filtered through a glass frit. The solvent was removed from the clear solution, the remaining pale yellow solid was washed with $Et_2O$ (2x15 mL) and dried at reduced pressure to afford **3** as a colourless solid (0.64 g, 90%), m.p. 230-240 °C (decomposes without melting). **$^1$H NMR** (400 MHz, $CDCl_3$, 294 K): $\delta$ 2.00-3.60 [m, 44H, overlapped resonances for H-6 – H-9, isomers **3a** + **3b**; H-10 ($\delta$ 2.22 ppm, s, **3b**), H-10 ($\delta$ 2.27 ppm, s, **3a**), H-5e ($\delta$ 2.78 ppm, d, $^2J_{H\text{-}5a,H\text{-}5e}$ = 13.0 Hz, **3a**), H-5e ($\delta$ 2.93 ppm, d, $^2J_{H\text{-}5a,H\text{-}5e}$ = 12.4 Hz, **3b**)], 4.42 (d, $^2J_{H\text{-}5a,H\text{-}5e}$ = 13.0 Hz, 4H, H-5a, **3a**), 4.75 (d, $^2J_{H\text{-}5a,H\text{-}5e}$ = 12.4 Hz, 4H, H-5a, **3b**), $AB_2$ spin system for **3a** with B at $\delta$ 6.58 ppm (d, $^3J_{H\text{-}3,H\text{-}4}$ = 7.3 Hz, 4H, H-3) and A at $\delta$ 6.71 ppm (t, $^3J_{H\text{-}3,H\text{-}4}$ = 7.3 Hz, 2H, H-4), $AB_2$ spin system for **3b** with B at $\delta$ 7.06 ppm (d, $^3J_{H\text{-}3,H\text{-}4}$ = 7.3 Hz, 4H, H-3) and A at $\delta$ 7.15 ppm (t, $^3J_{H\text{-}3,H\text{-}4}$ = 7.3 Hz, 2H, H-4). **$^{13}$C{$^1$H} NMR** (101 MHz, $CDCl_3$, 295 K): $\delta$ 46.06 (C-10, **3b**), 46.15 (C-10, **3a**), 52.49 (C-6 and C-8, **3a** + **3b**), 54.46 (C-7 and C-9, **3b**), 54.78 (C-7 and C-9, **3a**), 62.98 (C-5, **3b**), 63.09 (C-5, **3a**), 125.42 (C-3, **3a**), 126.11 (C-3, **3b**), 127.32 (C-4, **3a**), 127.51 (C-4, **3b**), 144.32 (C-2, **3a**), 145.75 (C-2, **3b**), 156.28 (C-1, **3a**), 157.96 (C-1, **3b**). **MS** (APCI+, MeOH): *m/z* (%) 879.28 (<1) $[M+H]^+$, 453.16 (100) $[RSb+MeO]^+$. HRMS (APCI+): Calc. for $[C_{36}H_{59}N_8O_2Sb_2]^+$ 879.28358. Found: 879.28599.

**Synthesis of *cyclo*-[2,6-$\{MeN(CH_2CH_2)_2NCH_2\}_2C_6H_3]_2Bi_2O_2$ (4).** A reaction mixture of **2** (0.20 g, 0.34 mmol) and KOH (1.00 g, 17.82 mmol) in toluene (30 mL) was stirred at reflux for 24h after which the excess KOH was filtered off and the residue was extracted with hot toluene. The combined extracts were concentrated and kept at −30 °C overnight to give the title compound as a colourless solid (0.17 g, 94%), m.p. 167 °C (decomposes without melting). **$^1$H NMR** (301 MHz, $CDCl_3$, 294 K): $\delta$ 1.70-3.35 [m, 44H, overlapped resonances for H-6 – H-9 with H-10 ($\delta$ 2.26 ppm) and H-5e (δ 3.00 ppm, d, $^2J_{H\text{-}5a,H\text{-}5e}$ = 12.6 Hz, 4H)], 4.53 (d, $^2J_{H\text{-}5a,H\text{-}5e}$ = 12.9 Hz, 4H, H-5a), 6.80-7.00 (s br, 6H, H-3 and H-4). **$^1$H NMR** (301 MHz, $CDCl_3$, 213 K): $\delta$ 1.71-1.88 (m, 8H, H-8a or H-8e and H-9a), 2.17-2.38 [m, 20H, overlapped resonances for H-6a and H-7e with H-10 ($\delta$ 2.27 ppm, s)], 2.38-2.49 (m, 4H, H-8a or H-8e), 2.51-2.66 (m, 4H, H-9e), 2.87 (d, $^2J_{H\text{-}7a,H\text{-}7e}$ = 9.3 Hz, 4H, H-7a), 2.99 (d, $^2J_{H\text{-}5a,H\text{-}5e}$ = 12.5 Hz, 4H, H-5e), 3.36 (d, $^2J_{H\text{-}6a,H\text{-}6e}$ = 9.9 Hz, 4H, H-6e), 4.40 (d, $^2J_{H\text{-}5a,H\text{-}5e}$ = 12.5 Hz, 4H, H-5a), 6.80-6.89 (m, 6H, H-3 and H-4). **$^{13}$C{$^1$H} NMR** (76 MHz, $CDCl_3$, 213 K): $\delta$ 46.07 (C-10), 51.26 (C-88), 54.10 (C-6), 54.75 (C-9), 56.10 (C-7), 64.82 (C-5), 126.77 (C-4), 127.61 (C-3), 147.69 (C-2), 198.43 (C-1). **MS** (ESI+, MeOH): *m/z* (%) 1053.43 (1<) $[M+H]^+$, 541.24 (100) $[RBi+MeO]^+$, 527.22 (74) $[RBiO+H]^+$, 303.25

(12) $[R+2H]^+$. HRMS (ESI+): Calc. for $[C_{36}H_{59}Bi_2N_8O_2]^+$: 1053.43632. Found: 1053.43272.

**Synthesis of [*cyclo*-{2-(MeN(H){$CH_2CH_2$}$_2$$NCH_2$)-6-(MeN{$CH_2CH_2$}$_2$$NCH_2$)$C_6H_3$}$_2$$Sb_2O(OH)$][$(O_2CCF_3)_3$] (5).** $CF_3C(O)OH$ (0.10 g, 0.92 mmol) was added *via* syringe over a solution of the oxide **3** (0.20 g, 0.23 mmol) in $CH_2Cl_2$ (40 mL). The resulting solution was stirred at room temperature overnight. The solvent was removed at reduced pressure to afford a pale yellow solid. This solid was dissolved in $CHCl_3$ and the solution filtered to remove insoluble product. Removal of the solvent from the clear solution gave **5** as a white-yellowish solid (0.24 g, 86%), m.p. 160-165 °C. **$^1$H NMR** (600 MHz, $CDCl_3$, 297 K) $\delta$ 2.25-2.85 (s br, 24H, H-10, isomer **5a** and H-10, isomer **5b**), 2.85-3.70 (m, 68H, H-6 − H-9, **5a**; H-6 − H-9, **5b**, and H-5e, **5b**), 3.94 (d, $^2J_{H\text{-}5a,H\text{-}5e}$ = 12.0 Hz, 4H, H-5e, **5a**), 4.13 (d, $^2J_{H\text{-}5a,H\text{-}5e}$ = 12.4 Hz, 4H, H-5a, **5a**), 4.22 (d, $^2J_{H\text{-}5a,H\text{-}5e}$ = 10.5 Hz, 4H, H-5a, **5b**), $AB_2$ spin system for **5b** with B at $\delta$ 6.79 ppm (d, $^3J_{H\text{-}3,H\text{-}4}$ = 7.4 Hz, 4H, H-3) and A at $\delta$ 6.95 ppm (t, $^3J_{H\text{-}3,H\text{-}4}$ = 7.5 Hz, 2H, H-4), $AB_2$ spin system for **5a** with B at $\delta$ 7.29 ppm (d, $^3J_{H\text{-}3,H\text{-}4}$ = 7.6 Hz, 4H, H-3) and A at $\delta$ 7.46 ppm (t, $^3J_{H\text{-}3,H\text{-}4}$ = 7.5 Hz, 2H, H-4). **$^{13}$C{$^1$H} NMR** (151 MHz, $CDCl_3$, 296 K): $\delta$ 44.16 (br, C-10, **5b**, and C-10, **5a**), 52.17 (br, C-6 and C-8, **5a** and **5b**), 52.81 (br, C-7 and C-9, **5a** and **5b**), 62.70 (br, C-5, **5b**), 64.37 (C-5, **5a**), 116.73 (q, $^1J_{C,F}$ = 292.6 Hz, *C*$F_3$), 126.33 (overlapped resonances of C-3, **5a** and C-3, **5b**), 130.24 (C-4, **5b**), 132.39 (br, C-4, **5a**), 143.43 (br, C-2, **5b**), 143.81 (C-2, **5a**), 147.02 (br, C-1, **5a**), 150.85 (C-1, **5b**), 162.66 (q, $^2J_{C,F}$ = 34.0 Hz, *C*OO). **$^{19}$F NMR** (565 MHz, $CDCl_3$, 296 K): $\delta$ −75.42. **IR** (KBr pellet, $\upsilon$, $cm^{-1}$): 1693 (s) ($CO_2$). **MS** (ESI+, MeCN): 439.15 (100) $[RSbOH]^+$, 421.13 (15) $[RSb\text{-}H]^+$, 300.23 (40) $[R\text{-}H]^+$. HRMS (ESI+): Calc. for $[RSbOH]^+$ 439.14523. Found: 439.14365.

**Synthesis of "[2,6-{MeN($CH_2CH_2$)$_2$$NCH_2$}$_2$$C_6H_3$]$SbCO_3$" (6).** $CO_2$ was bubbled in a solution of the oxide **3** (0.30 g, 0.34 mmol) in $CHCl_3$ (30 mL) for 3h. The solvent evaporated during this time, affording **6** as a colourless solid (0.32 g, 100%), m.p. 230-240 °C (decomposes without melting). **$^1$H NMR** (400 MHz, $CDCl_3$, 295 K): $\delta$ 2.30-2.45 [m, 10H, overlapped resonances for H-8a ($\delta$ ~2.37 ppm, m) and H-9a ($\delta$ ~2.40 ppm, m) with H-10 ($\delta$ 2.37 ppm, s)], 2.56 (td, $^2J_{H\text{-}7a,H\text{-}7e} \approx {}^3J_{H\text{-}7a,H\text{-}6a}$ = 11.4 Hz, $^3J_{H\text{-}7a,H\text{-}6e}$ = 3.0 Hz, 2H, H-7a), 2.65-2.90 (m, 8H, overlapped resonances of H-7e $\delta$ ~2.84 ppm, H-6a $\delta$ ~2.78 ppm, H-8e $\delta$ ~2.76 ppm, H-9e $\delta$ ~2.72 ppm), 3.44 (d, $^2J_{H\text{-}5a,H\text{-}5e}$ = 14.2 Hz, 2H, H-5e), 3.53 (d, $^2J_{H\text{-}6a,H\text{-}6e}$ = 11.2 Hz, 2H, H-6e), 4.39 (d, $^2J_{H\text{-}5a,H\text{-}5e}$ = 14.2 Hz, 2H, H-5a), $AB_2$ spin system with B at $\delta$ 7.17 ppm (d, $^3J_{H\text{-}3,H\text{-}4}$ = 7.5 Hz, 2H, H-3) and A at $\delta$ 7.34 ppm (t, $^3J_{H\text{-}3,H\text{-}4}$ = 7.5 Hz, 1H, H-4). **$^{13}$C{$^1$H} NMR** (101 MHz, $CDCl_3$, 295 K): $\delta$ 46.07 (C-10), 51.86 (C-8), 53.29 (C-9), 53.84 (C-6), 54.67 (C-7), 62.77 (br, C-5), 126.12 (C-3), 131.22 (C-4), 145.45 (C-2), 146.04 (C-1), 161.00 (C-11). **IR** (KBr pellet, $\upsilon$, $cm^{-1}$): 1692 (s), 1678 (s), 1640 (s) ($CO_3$). **MS** (ESI+, MeOH): 877.28 (2) $[R_2Sb_2O_2+H]^+$, 481.16 (6) $[RSb+MeO+CO]^+$, 453.16 (2) $[RSb+MeO]^+$, 439.15 (100) $[M-CO_2+H]^+$. HRMS (ESI+): Calc. for $[C_{20}H_{32}N_4O_2Sb]^+$ 481.15580. Found: 481.15469.

**Synthesis of "[2,6-{MeN($CH_2CH_2$)$_2$$NCH_2$}$_2$$C_6H_3$]$BiCO_3$" (7).** $CO_2$ was bubbled in a solution of oxide **4** (0.50 g, 0.47 mmol) in $CHCl_3$ (30 mL) for 2h. After evaporation of the solvent using a rotary evaporator and drying the compound at 45 °C under reduced pressure (10 mbar), **7** was obtained as a colourless solid. (0.54 g, 100%), m.p. 150-160 °C (decomposes without melting). **$^1$H NMR** (400 MHz, $CDCl_3$, 295 K): $\delta$ 2.14 (dd, $^2J_{H\text{-}9a,H\text{-}9e} \approx {}^3J_{H\text{-}8a,H\text{-}9a}$ = 11.4 Hz, 2H, H-9a), 2.30-2.43 [m, 8H, overlapped resonances for H-7a ($\delta$ ~2.37 ppm, m) and H-10 ($\delta$ ~2.37 ppm, s)], 2.54 (dd, $^2J_{H\text{-}8a,H\text{-}8e} \approx {}^3J_{H\text{-}8a,H\text{-}9a}$ = 11.9 Hz, 2H, H-8a), 2.71-2.86 (m, 6H, overlapped resonances for H-6a, H-8e and H-9e), 2.97 (d, $^2J_{H\text{-}7a,H\text{-}7e}$ = 12.5 Hz, 2H, H-7e), 3.55 (d, $^2J_{H\text{-}6a,H\text{-}6e}$ = 11.7 Hz, 2H, H-6e), 3.96 (d, $^2J_{H\text{-}5a,H\text{-}5e}$ = 14.1 Hz, 2H, H-5e), 4.46 (d, $^2J_{H\text{-}5a,H\text{-}5e}$ = 14.1 Hz, 2H, H-5a), $A_2B$ spin system with B at $\delta$ 7.45 ppm (t, $^3J_{H\text{-}3,H\text{-}4}$ = 7.4 Hz, 1H, H-4) and A at $\delta$ 7.56 ppm (d, $^3J_{H\text{-}3,H\text{-}4}$ = 7.5 Hz, 2H, H-3). **$^{13}$C{$^1$H} NMR** (101 MHz, $CDCl_3$, 295 K): $\delta$ 45.98 (C-10), 51.98 (C-8), 54.31 (C-6), 54.79 (C-9), 56.32 (C-7), 65.87 (C-5), 128.27 (C-3), 130.34 (C-4), 150.84 (C-2), 162.86 (C-11), 195.04 (C-1). **IR** (KBr pellet, $\upsilon$, $cm^{-1}$): 1698 (sh), 1663 (s), 1631 (s) ($CO_3$). **MS** (ESI+, MeOH): 541.24 (100) $[RBi+MeO]^+$, 300.23 (34) $[R\text{-}H]^+$. HRMS (ESI+): Calc. for $[C_{19}H_{32}N_4OBi]^+$ 541.23745. Found: 541.23610.

**Synthesis of [2,6-{MeN($CH_2CH_2$)$_2$$NCH_2$}$_2$$C_6H_3$]Sb[O(O)CC(O)O] (8).** Oxalic acid dihydrate (0.06 g, 0.46 mmol) was added to a solution of **3** (0.20 g, 0.23 mmol) in ethanol (25 mL). The reaction mixture, which became a colourless solution after the addition of the acid, was heated for 3 h at 55 °C, then left to reach room temperature. The solution was dried over anh. $Na_2SO_4$, then filtered and the solvent was removed at reduced pressure to afford **8** as a colourless solid (0.22 g, 96%), m.p. 215-220 °C. **$^1$H NMR** (400 MHz, $CDCl_3$, 296 K): $\delta$ 2.22-2.42 [s br, 10H, overlapped resonances for H-9a ($\delta$ ~2.34 ppm) and H-8a ($\delta$ ~2.35 ppm) with H-10 ($\delta$ 2.35 ppm)], 2.50 (dd, $^2J_{H\text{-}7a,H\text{-}7e} \approx {}^3J_{H\text{-}6a,H\text{-}7a}$ = 10.5 Hz, 2H, H-7a), 2.60-2.90 [m, 8H, overlapped resonances for H-8e ($\delta$ ~2.66 ppm), H-9e ($\delta$ ~2.70 ppm), H-6a ($\delta$ ~2.76 ppm), and H-7e ($\delta$ ~2.84 ppm)], 3.34 (d, $^2J_{H\text{-}5a,H\text{-}5e}$ = 13.4 Hz, 2H, H-5e), 3.72 (d, $^2J_{H\text{-}6a,H\text{-}6e} \approx {}^3J_{H\text{-}6a,H\text{-}7a}$ = 10.6 Hz, 2H, H-6e), 4.44 (d, $^2J_{H\text{-}5a,H\text{-}5e}$ = 14.1 Hz, 2H, H-5a), $AB_2$ spin system with B at $\delta$ 7.16 ppm (d, $^3J_{H\text{-}3,H\text{-}4}$ = 7.0 Hz, 2H, H-3) and A at $\delta$ 7.34 ppm (t, $^3J_{H\text{-}3,H\text{-}4}$ = 7.0 Hz, 1H, H-4). **$^{13}$C{$^1$H} NMR** (101 MHz, $CDCl_3$, 297 K): $\delta$ = 46.22 (C-10), 51.42 (C-8), 53.28 (br, C-9), 53.55 (C-6), 54.53 (br, C-7), 62.09 (br, C-5), 126.75 (C-3), 131.76 (C-4), 145.53 (C-2), 146.83 (C-1), 162.07 (C-11). **IR** (KBr pellet, $\upsilon$, $cm^{-1}$): 1719 (s), 1597 (s) ($CO_2$). **MS** (ESI+, MeOH): *m/z* (%) 549.08 (6) $[M+K]^+$, 533.11 (8) $[M+Na]^+$, 511.13 (100) $[M+H]^+$, 453.16 (99) $[RSb+MeO]^+$ 439.14 (36) $[RSb+OH]^+$, 423.15 (24) $[RSb+H]^+$. HRMS (ESI+): Calc. for $[C_{20}H_{30}N_4O_4Sb]^+$ 511.12997. Found 511.12929.

**Synthesis of [(2,6-{MeN($CH_2CH_2$)$_2$$NCH_2$}$_2$$C_6H_3$]Sb[$O_2$-1,2-$C_6H_3$-3-$(CH_2)_2NH_3$]Cl (9).** Dopamine chlorhidrate (0.09 g, 0.46 mmol) was added over a solution of the oxide **3** (0.20 g, 0.23 mmol) in ethanol (25 mL). The reaction mixture was



 

stirred for 24 h at room temperature, then the solvent was removed *in vacuo*. The remaining pale yellow solid was dissolved in $CH_2Cl_2$, the solution was dried over anh. $Na_2SO_4$, then filtered through a glass frit. The solvent was removed from the clear solution under reduced pressure and the remaining yellow solid was washed with $Et_2O$ (2x10 mL) to give **9** as a pale yellow solid (0.27 g, 96%), m.p. 210-220 °C (melts with decomposition). **$^1$H NMR** (600 MHz, $CDCl_3$, 296 K): $\delta$ 2.15-2.40 [m, 10H, overlapped resonances for H-8a, H-9a, H-8′a and H-9′a with H-10 ($\delta$ 2.32 or 2.34 ppm, s) and H-10′ ($\delta$ 2.32 or 2.34 ppm, s)], 2.45-2.70 (m, 8H, overlapped resonances for H-6a, H-6′a, H-7a, H-7′a, H-8e, H-8′e, H-9e, H-9′e), 2.72 (t, $^3J_{H-17,H-18}$ = 7.1 Hz, 2H, H-17), 2.78-2.88 (m, 2H, H-7e and H-7′e), 2.93-3.03 (m, 2H, H-18), 3.03-3.14 (m, 2H, H-5e and H-5′e), 3.61-3.86 (m br, 2H, H-6e and H-6′e), 4.46 (d, $^2J_{HH}$ = 13.7 Hz, H-5′a or H-5a) overlapped with 4.47 (d, $^2J_{HH}$ = 13.8 Hz, H-5a or H-5′a), 4.73 (s br, 3H, N$H_3$), 6.28 (dd, $^3J_{H-14,H-15}$ = 7.8 Hz, $^4J_{H-12,H-14}$ = 2.1 Hz, 1H, H-14), 6.47 (d, $^4J_{H-12,H-14}$ = 2.1 Hz, 1H, H-12), 6.51 (d, $^3J_{H-14,H-15}$ = 7.8 Hz, 1H, H-15), 6.97 (d, $^3J_{H-3′ \text{ or } H-3,H-4}$ = 7.4 Hz, 1H, H-3′ or H-3), 6.99 (d, $^3J_{H-3 \text{ or } H-3′,H-4}$ = 7.4 Hz, 1H, H-3 or H-3′), 7.10 (dd, $^3J_{H-3,H-4}$ = $^3J_{H-3′,H-4}$ = 7.4 Hz, 1H, H-4). **$^{13}$C{$^1$H} NMR** (151 MHz, $CDCl_3$, 298 K): $\delta$ 34.28 (C-17), 41.88 (C-18), 46.04 (C-10 or C-10′), 46.06 (C-10′ or C-10), 51.51 (C-8 and C-8′), 53.44 (C-6 and C-6′), 53.67 (C-9 and C-9′), 54.97 (C-7 and C-7′), 62.33 (C-5 and C-5′), 113.89 (C-15), 114.51 (C-12), 118.03 (C-14), 125.72 (C-13), 126.38 (C-3 or C-3′), 126.46 (C-3′ or C-3), 129.85 (C-4), 145.82 (C-2 or C-2′), 145.88 (C-2′ or C-2), 149.80 (C-1), 151.98 (C-16), 153.13 (C-11). **MS** (APCI+, MeOH): *m/z* (%) 574.21 (100) $[M-Cl]^+$, 457.11 (10) $[RSb+Cl]^+$. HRMS (APCI+): Calc. for $[C_{26}H_{39}N_5O_2Sb]^+$ 574.21364. Found: 574.21496.

**Synthesis of [2,6-{MeN(CH$_2$CH$_2$)$_2$NCH$_2$}$_2$C$_6$H$_3$]Sb(OCH$_2$)$_2$ (10).** A solution of KOH (0.07 g, 1.22 mmol) in ethanol (25 mL) was added over a solution of **1** (0.30 g, 0.61 mmol) and ethylene glycol (0.04 g, 0.61 mmol), in ethanol (15 mL). The reaction mixture was stirred for 24 h at room temperature, then the solvent was removed *in vacuo*. The remaining solid was dissolved in $CH_2Cl_2$, the solution was dried over anh. $Na_2SO_4$, then filtered through a glass frit. The solvent was removed from the clear colourless solution and the remaining solid was dissolved in $Et_2O$ (20 mL) and filtered again. Evaporation of the solvent gave **10** as a colourless solid (0.25 g, 86%), m.p. 135-140 °C. **$^1$H NMR** (600 MHz, $CDCl_3$, 295 K): $\delta$ 1.81-2.90 [m, 22H, overlapped resonances for H-6 – H-9 with H-10 ($\delta$ 2.30 ppm, s)], 2.95 (d, $^2J_{H-5a,H-5e}$ = 13.2 Hz, 2H, H-5e), 3.43-3.53 (m, AA′BB′ vicinal spin system, 2H, H-11a), 3.67-3.82 (m, AA′BB′ vicinal spin system, 2H, H-11e), 4.48 (d, $^2J_{H-5a,H-5e}$ = 13.2 Hz, 2H, H-5a), $AB_2$ spin system with B at $\delta$ 7.02 ppm (d, $^3J_{H-3,H-4}$ = 7.5 Hz, 2H, H-3) and A at $\delta$ 7.14 ppm (t, $^3J_{H-3,H-4}$ = 7.4 Hz, 1H, H-4). **$^{13}$C{$^1$H} NMR** (151 MHz, $CDCl_3$, 295 K): $\delta$ 46.11 (C-10), 51.65 (br, C-6 and C-8), 54.40 (br, C-7 and C-9), 62.49 (C-5), 66.85 (C-11), 126.33 (C-3), 128.79 (C-4), 146.02 (C-2), 150.95 (C-1). **$^1$H NMR** (301 MHz, $CDCl_3$, 213 K): $\delta$ 2.06 (dd, $^2J_{H-8a,H-8e} \approx {}^3J_{H-8a,H-9a}$ = 11.1 Hz, 2H, H-8a), 2.21 (dd, $^2J_{H-9a,H-9e} \approx {}^3J_{H-8a,H-9a}$ = 11.2 Hz, 2H, H-9a), 2.32 (s, 6H, H-10), 2.35-2.50 (m, 4H, overlapped resonances of H-6a at $\delta$ ~2.40 ppm and H-7a at $\delta$ ~2.44 ppm), 2.50-2.70 (m, 4H, overlapped resonances of H-8e at $\delta$ ~2.56 ppm and H-9e at $\delta$ ~2.63 ppm), 2.82 (d, $^2J_{H-7a,H-7e}$ = 8.9 Hz, 2H, H-7e), 2.92 (d, $^2J_{H-5a,H-5e}$ = 13.3 Hz, 2H, H-5e), 3.36 (d, $^2J_{H-6a,H-6e}$ = 8.4 Hz, 2H, H-6e), 3.40-3.51 (m br, AA′BB′ vicinal spin system, 2H, H-11a), 3.64-3.76 (m br, AA′BB′ vicinal spin system, 2H, H-11e), 4.43 (d, $^2J_{H-5a,H-5e}$ = 13.2 Hz, 2H, H-5a), $AB_2$ spin system with B at $\delta$ 7.01 ppm (d, $^3J_{H-3,H-4}$ = 7.2 Hz, 2H, H-3) and A at $\delta$ 7.13 ppm (t, $^3J_{H-3,H-4}$ = 7.2 Hz, 1H, H-4). **$^{13}$C{$^1$H} NMR** (76 MHz, $CDCl_3$, 213 K): $\delta$ 46.02 (C-10), 51.24 (C-8), 53.01 (C-6), 53.56 (C-9), 54.86 (C-7), 62.31 (C-5), 66.39 (C-11), 126.16 (C-3), 128.68 (C-4), 145.58 (C-2), 149.93 (C-1). **$^1$H NMR** (301 MHz, $CDCl_3$, 333 K): $\delta$ 2.31 (s, 6H, H-10), 2.35-2.91 (m br, 16H, H-6 – H-9), 2.95 (d, $^2J_{H-5a,H-5e}$ = 13.2 Hz, 2H, H-5e), 3.47-3.57 (m, AA′BB′ vicinal spin system, 2H, H-11a), 3.68-3.81 (m, AA′BB′ vicinal spin system, 2H, H-11e), 4.52 (d, $^2J_{H-5a,H-5e}$ = 13.2 Hz, 2H, H-5a), $AB_2$ spin system with B at $\delta$ 7.02 ppm (d, $^3J_{H-3,H-4}$ = 7.4 Hz, 2H, H-3) and A at $\delta$ 7.14 ppm (t, $^3J_{H-3,H-4}$ = 7.4 Hz, 1H, H-4). **$^{13}$C{$^1$H} NMR** (76 MHz, $CDCl_3$, 333 K): $\delta$ 46.11 (C-10), 52.45 (C-6 and C-8), 54.65 (C-7 and C-9), 62.60 (C-5), 67.08 (C-11), 126.36 (C-3), 128.75 (C-4), 146.23 (C-2), 151.54 (C-1). **MS** (APCI+, MeOH): *m/z* (%) 483.17 (28) $[M+H]^+$, 453.16 (100) $[RSb+MeO]^+$. HRMS (APCI+): Calc. for $[C_{20}H_{34}N_4O_2Sb]^+$ 483.17145. Found: 483.17068.

**Synthesis of [2,6-{MeN(CH$_2$CH$_2$)$_2$NCH$_2$}$_2$C$_6$H$_3$]Bi(OCH$_2$)$_2$ (11).** A reaction mixture of **2** (0.20 g, 0.34 mmol), ethylene glycol (0.02 g, 0.34 mmol) and KOH (0.08 g, 1.36 mmol) in ethanol (25 mL) was stirred for 24 h at room temperature, then the solvent was removed *in vacuo* and the solid residue was extracted with $Et_2O$. Evaporation of the solvent from the resulting clear solution yielded **11** as a colourless solid (0.18 g, 95%), m.p. 172 °C. **$^1$H NMR** (301 MHz, $CDCl_3$, 293 K): $\delta$ 1.86-3.65 [m, 22H, overlapped resonances for H-6 – H-9 with H-10 ($\delta$ 2.31 ppm, s) and H-5e ($\delta$ 3.18 ppm, d, $^2J_{H-5a,H-5e}$ = 13.2 Hz, 2H)], 4.12-4.25 (m, AA′BB′ vicinal spin system, 2H, H-11a), 4.45-4.58 [m, AA′BB′ vicinal spin system, 4H, overlapped resonances for H-11e with H-5a (d, $^2J_{H-5a,H-5e}$ = 13.2 Hz)], $A_2B$ spin system with B at $\delta$ 7.25 ppm (t, $^3J_{H-3,H-4}$ = 7.3 Hz, 1H, H-4) and A at $\delta$ 7.35 ppm (d, $^3J_{H-3,H-4}$ = 7.3 Hz, 2H, H-3). **$^{13}$C{$^1$H} NMR** (76 MHz, $CDCl_3$, 293 K): $\delta$ 46.15 (C-10), 51.43 (C-8), 53.41 (C-6), 54.95 (C-9), 56.45 (C-7), 64.11 (C-5), 71.38 (C-11), 128.24 (C-4), 128.58 (C-3), 149.90 (C-2), 196.86 (C-1). **$^1$H NMR** (400 MHz, $CDCl_3$, 223 K): $\delta$ 1.96 (dd, $^2J_{H-9a,H-9e} \approx {}^3J_{H-8a,H-9a}$ = 11.1 Hz, 2H, H-9a), 2.12-2.37 [m, 12H, overlapped resonances for H-6a, H-7e and H-8a with H-10 ($\delta$ 2.29 ppm, s)], 2.61 (d, $^2J_{H-8a,H-8e}$ = 11.2 Hz, 2H, H-8e), 2.69 (d, $^2J_{H-9a,H-9e}$ = 11.2 Hz, 2H, H-9e), 2.91 (d, $^2J_{H-7a,H-7e}$ = 7.4 Hz, 2H, H-7a), 3.16 (d, $^2J_{H-5a,H-5e}$ = 13.2 Hz, 2H, H-5e), 3.35 (d, $^2J_{H-6a,H-6e}$ = 7.0 Hz, 2H, H-6e), 4.04-4.13 (m, AA′BB′ vicinal spin system, 2H, H-11a), 4.36-4.50 (m, 4H, overlapped resonances for AA′BB′ vicinal spin system for H-11e with H-5a), $A_2B$ spin system with B at $\delta$ 7.21 ppm (t, $^3J_{H-3,H-4}$ = 7.3 Hz, 1H, H-4) and A at $\delta$ 7.32 ppm (d, $^3J_{H-3,H-4}$ = 7.3 Hz, 2H, H-3). **$^{13}$C{$^1$H} NMR** (101 MHz, $CDCl_3$, 223 K): $\delta$ 46.02 (C-10), 51.14 (C-8), 53.10

(C-6), 54.60 (C-9), 56.08 (C-7), 63.79 (C-5), 70.71 (C-11), 128.13 (C-4), 128.38 (C-3), 149.49 (C-2), 195.85 (C-1). **MS** (APCI+, MeOH): *m/z* (%) 571.25 (100) $[M+H]^+$, 509.21 (12) $[M–O_2C_2H_4]^+$, 303.25 (23) $[R+2H]^+$. HRMS (APCI+): Calc. for $[C_{20}H_{34}BiN_4O_2]^+$: 571.24801. Found: 571.24724.

**Synthesis of [2,6-{MeN(CH$_2$CH$_2$)$_2$NCH$_2$}$_2$C$_6$H$_3$]Sb(OCMe$_2$)$_2$ (12).** Prepared as described for **10** from **1** (0.20 g, 0.40 mmol), pinacol (0.05 g, 0.4 mmol) and KOH (0.04 g, 0.80 mmol) in ethanol (50 mL). Work-up of the reaction mixture (see ESI†) gave **12** as a colourless solid (0.16 g, 73%), m.p. 155-160 °C. **$^1$H NMR** (600 MHz, $CDCl_3$, 295 K): $\delta$ 0.72 (s, 6H, H-12), 1.05 (s, 6H, H-13), 2.33 (s, 6H, H-10), 2.25-2.71 (m, 16H, overlapped resonances for H-6 – H-9), 2.93 (d, $^2J_{H\text{-}5a,H\text{-}5e}$ = 13.0 Hz, 2H, H-5e), 4.56 (d, $^2J_{H\text{-}5a,H\text{-}5e}$ = 13.0 Hz, 2H, H-5a), $AB_2$ spin system with B at $\delta$ 7.00 ppm (d, $^3J_{H\text{-}3,H\text{-}4}$ = 7.5 Hz, 2H, H-3) and A at $\delta$ 7.12 ppm (t, $^3J_{H\text{-}3,H\text{-}4}$ = 7.4 Hz, 1H, H-4). **$^{13}$C{$^1$H} NMR** (151 MHz, $CDCl_3$, 295 K): $\delta$ 25.95 (C-12), 26.69 (C-13), 46.22 (C-10), 52.39 (br, C-6 and C-8), 54.54 (br, C-7 and C-9), 62.90 (C-5), 77.55 (C-11), 126.07 (C-3), 128.14 (C-4), 145.70 (C-2), 153.22 (C-1). **$^1$H NMR** (301 MHz, $CDCl_3$, 213 K): $\delta$ 0.65 (s, 6H, H-12), 1.00 (s, 6H, H-13), 2.05 (dd, $^2J_{H\ 8a,H\ 8e} \approx {}^3J_{H\ 8a,H\ 9a}$ = 11.5 Hz, 2H, H-8a), 2.18-2.40 [m, 10H, overlapped resonances for H-9a ($\delta$ ~2.26 ppm, d, $^2J_{H\text{-}9a,H\text{-}9e}$ = 11.3 Hz) and H-6a ($\delta$ ~2.35 ppm) with H-10 ($\delta$ 2.34 ppm, s)], 2.46 (dd, $^2J_{H\text{-}7a,H\text{-}7e} \approx {}^3J_{H\text{-}6a,H\text{-}7a}$ = 11.0 Hz, 2H, H-7a), 2.58 (d, $^2J_{H\text{-}8a,H\text{-}8e}$ = 12.3 Hz, 2H, H-8e), 2.62 (d, $^2J_{H\text{-}9a,H\text{-}9e}$ = 11.8 Hz, 2H, H-9e), 2.83 (d, $^2J_{H\text{-}7a,H\text{-}7e}$ = 11.0 Hz, 2H, H-7e), 2.91 (d, $^2J_{H\text{-}5a,H\text{-}5e}$ = 13.1 Hz, 2H, H-5e), 3.52 (d, $^2J_{H\text{-}6a,H\text{-}6e}$ = 10.4 Hz, 2H, H-6e), 4.51 (d, $^2J_{H\text{-}5a,H\text{-}5e}$ = 13.0 Hz, 2H, H-5a), $AB_2$ spin system with B at $\delta$ 7.01 ppm (d, $^3J_{H\text{-}3,H\text{-}4}$ = 7.4 Hz, 2H, H-3) and A at $\delta$ 7.13 ppm (t, $^3J_{H\text{-}3,H\text{-}4}$ = 7.4 Hz, 1H, H-4). **$^{13}$C{$^1$H} NMR** (76 MHz, $CDCl_3$, 213 K): $\delta$ 25.65 (C-12), 26.43 (C-13), 46.05 (C-10), 51.12 (C-8), 53.03 (C-6), 53.55 (C-9), 54.87 (C-7), 62.61 (C-5), 77.11 (C-11), 125.89 (C-3), 127.92 (C-4), 145.28 (C-2), 152.46 (C-1). **$^1$H NMR** (301 MHz, $CDCl_3$, 333 K): $\delta$ 0.75 (s, 6H, H-12), 1.08 (s, 6H, H-13), 2.33 (s, 6H, H-10), 2.42-3.00 (m, 18H, overlapped resonances for H-6 – H-9 with H-5e ($\delta$ 2.94 ppm, d, $^2J_{H\text{-}5a,H\text{-}5e}$ = 13.0 Hz)], 4.58 (d, $^2J_{H\text{-}5a,H\text{-}5e}$ = 13.1 Hz, 2H, H-5a), $AB_2$ spin system with B at $\delta$ 7.01 ppm (d, $^3J_{H\text{-}3,H\text{-}4}$ = 7.4 Hz, 2H, H-3) and A at $\delta$ 7.12 ppm (t, $^3J_{H\text{-}3,H\text{-}4}$ = 7.4 Hz, 1H, H-4). **$^{13}$C{$^1$H} NMR** (76 MHz, $CDCl_3$, 333 K): $\delta$ 26.02 (C-12), 26.74 (C-13), 46.20 (C-10), 52.55 (C-6 or C-8), 54.65 (C-7 and C-9), 63.02 (C-5), 77.77 (C-11), 126.15 (C-3), 128.21 (C-4), 145.88 (C-2), 153.56 (C-1). **MS** (APCI+, MeOH): *m/z* (%) 539.23 (100) $[M+H]^+$. HRMS (APCI+): Calc. for $[C_{24}H_{42}N_4O_2Sb]^+$ 539.23405. Found: 539.23350.

**Synthesis of [2,6-{MeN(CH$_2$CH$_2$)$_2$NCH$_2$}$_2$C$_6$H$_3$]Bi(OCMe$_2$)$_2$ (13).** Prepared as described for **11** from **2** (0.20 g, 0.34 mmol), pinacol (0.04 g, 0.34 mmol) and KOH (0.08 g, 1.36 mmol) in ethanol (25 mL). Work-up of the reaction mixture (see ESI†) gave **13** as a colourless solid (0.19 g, 89%), m.p. 176 °C. **$^1$H NMR** (400 MHz, $CDCl_3$, 293 K): $\delta$ 0.73 (s, 6H, H-12 or H-13), 1.05 (s, 6H, H-13 or H-12), 1.80-3.81 [m br, 22H, overlapped resonances for H-6 – H-9 with H-10 ($\delta$ 2.33 ppm) and H-5e ($\delta$ 3.12 ppm, d, $^2J_{H\text{-}5a,H\text{-}5e}$ = 12.9 Hz, 2H)], 4.59 (d, $^2J_{H\text{-}5a,H\text{-}5e}$ = 12.9 Hz, 2H, H-5a), $A_2B$ spin system with B at $\delta$ 7.21 ppm (t, $^3J_{H\text{-}3,H\text{-}4}$ = 7.3 Hz, 1H, H-4) and A at $\delta$ 7.29 ppm (d, $^3J_{H\text{-}3,H\text{-}4}$ = 7.3 Hz, 2H, H-3). **$^{13}$C{$^1$H} NMR** (101 MHz, $CDCl_3$, 293 K): $\delta$ 28.27 (C-12 or C-13), 28.65 (C-13 or C-12), 46.24 (C-10), 50.87-87.13 (C-6 – C-9) 64.19 (C-5), 79.36 (C-11), 127.54 (C-4), 128.26 (C-3), 149.42 (C-2), 195.86 (C-1). **$^1$H NMR** (301 MHz, $CDCl_3$, 233 K): $\delta$ 0.69 (s, 6H, H-12 or H-13), 1.02 (s, 6H, H-13 or H-12), 2.01 (dd, $^2J_{H\text{-}9a,H\text{-}9e} \approx {}^3J_{H\text{-}8a,H\text{-}9a}$ = 11.2 Hz, 2H, H-9a), 2.09-2.41 [m, 12H, overlapped resonances for H-6a, H-7e and H-8a or H-8e with H-10 ($\delta$ 2.34 ppm, s)], 2.51-2.81 (m, 4H, H-8a or H-8e, H-9e), 2.94 (d, $^2J_{H\text{-}7a,H\text{-}7e}$ = 10.1 Hz, 2H, H-7a), 3.13 (d, $^2J_{H\text{-}5a,H\text{-}5e}$ = 12.9 Hz, 2H, H-5e), 3.55 (d, $^2J_{H\text{-}6a,H\text{-}6e}$ = 10.3 Hz, 2H, H-6e), 4.56 (d, $^2J_{H\text{-}5a,H\text{-}5e}$ = 12.9 Hz, 2H, H-5a), $A_2B$ spin system with B at $\delta$ 7.22 ppm (t, $^3J_{H\text{-}3,H\text{-}4}$ = 7.1 Hz, 1H, H-4) and A at $\delta$ 7.30 ppm (d, $^3J_{H\text{-}3,H\text{-}4}$ = 7.1 Hz, 2H, H-3). **$^{13}$C{$^1$H} NMR** (76 MHz, $CDCl_3$, 233 K): $\delta$ 27.95 (C-12 or C-13), 28.30 (C-13 or C-12), 46.11 (C-10), 51.16 (C-8), 53.20 (C-6), 54.67 (C-9), 56.18 (C-7), 63.94 (C-5), 78.94 (C-11), 127.43 (C-4), 128.10 (C-3), 149.10 (C-2), 195.39 (C-1). **MS** (APCI+, MeOH): *m/z* (%) 627.31 (100) $[M+H]^+$, 510.22 (6) $[M–O_2C_2(CH_3)_4]^+$, 303.25 (5) $[R+2H]^+$. HRMS (APCI+): Calc. for $[C_{24}H_{42}BiN_4O_2]^+$ 627.31116. Found: 627.31091.

**Synthesis of [2,6-{MeN(CH$_2$CH$_2$)$_2$NCH$_2$}$_2$C$_6$H$_3$]Sb(O$_2$-1,2-C$_6$H$_4$) (14).** (a) Catechol (0.05 g, 0.46 mmol) was added over a solution of the oxide **3** (0.20 g, 0.23 mmol) in ethanol (20 mL). The reaction mixture was stirred for 24 h at room temperature, then the solvent was removed *in vacuo*. Diethyl ether (30 mL) was added over the remaining white solid and the mixture was filtered through a glass frit. The solvent was removed from the clear, colourless solution under reduced pressure to give **14** as a white solid solid (0.23 g, 96%).

(b) Prepared as described for **10** from **1** (0.13 g, 0.27 mmol), catechol (0.03 g, 0.26 mmol) and KOH (0.03 g, 0.52 mmol) in ethanol (30 mL). Work-up of the reaction mixture (see ESI†) gave **14** as a colourless crystalline solid (0.11 g, 79%), m.p. 225-230 °C. **$^1$H NMR** (600 MHz, $CDCl_3$, 295 K): $\delta$ 2.20-2.32 (m, 2H, H-8a), 2.33-2.45 [m, 8H, overlapped resonances for H-9a ($\delta$ ~2.43 ppm) with H-10 ($\delta$ 2.41 ppm)], 2.62-2.85 (m br, 8H, overlapped resonances of H-6a, H-7a, H-8e, H-9e), 2.94 (s br, 2H, H-7e), AB spin system with A at $\delta$ 3.09 ppm ($^2J_{H\text{-}5a,H\text{-}5e}$ = 13.0 Hz, 2H, H-5e) and B at $\delta$ 4.53 ppm ($^2J_{H\text{-}5a,H\text{-}5e}$ = 13.5 Hz, 2H, H-5a), 3.79 (s br, 2H, H-6e), 6.41-6.47 (m, AA′BB′ spin system, 2H, H-13), 6.58-6.64 (m, AA′BB′ spin system, 2H, H-12), $AB_2$ spin system with B at $\delta$ 7.01 ppm (d, $^3J_{H\text{-}3,H\text{-}4}$ = 7.4 Hz, 2H, H-3) and A at $\delta$ 7.14 ppm (t, $^3J_{H\text{-}3,H\text{-}4}$ = 7.4 Hz, 1H, H-4). **$^{13}$C{$^1$H} NMR** (151 MHz, $CDCl_3$, 297 K): $\delta$ 46.17 (C-10), 51.61 (C-8), 53.52 (C-6), 53.72 (C-9), 55.13 (C-7), 62.41 (C-5), 114.09 (C-12), 117.62 (C-13), 126.28 (C-3), 129.69 (C-4), 145.88 (C-2), 150.07 (C-1), 152.94 (C-11). **$^1$H NMR** (301 MHz, $CDCl_3$, 213 K): $\delta$ 2.17-2.37 [m, 4H, overlapped resonances for H-9a ($\delta$ ~2.35 ppm) and H-8a ($\delta$ ~2.23 ppm)], 2.41 (s, 6H, H-10), 2.51-2.64 [m, 4H, overlapped resonances of H-6a ($\delta$ ~2.56 ppm) and H-7a ($\delta$ ~2.58 ppm)], 2.66-2.81 [m, 4H, overlapped resonances for H-8e ($\delta$ 2.71 ppm, d, $^2J_{H\text{-}8a,H\text{-}8e}$ = 10.5 Hz) with H-9e ($\delta$ 2.75 ppm, d, $^2J_{H\text{-}9a,H\text{-}9e}$ = 10.6 Hz)], 2.96

(d, $^2J_{H\text{-}7a,H\text{-}7e}$ = 8.0 Hz, 2H, H-7e), AB spin system with A at $\delta$ 3.07 ppm ($^2J_{H\text{-}5a,H\text{-}5e}$ = 13.6 Hz, 2H, H-5e) and B at $\delta$ 4.50 ppm ($^2J_{H\text{-}5a,H\text{-}5e}$ = 13.5 Hz, 2H, H-5a), 3.79 (d, $^2J_{H\text{-}6a,H\text{-}6e}$ = 7.8 Hz, 2H, H-6a), 6.39-6.54 (m, AA′BB′ spin system, 2H, H-13), 6.59-6.70 (m, AA′BB′ spin system, 2H, H-12), $AB_2$ spin system with B at $\delta$ 7.01 ppm (d, $^3J_{H\text{-}3,H\text{-}4}$ = 7.3 Hz, 2H, H-3) and A at $\delta$ 7.12 ppm (t, $^3J_{H\text{-}3,H\text{-}4}$ = 7.3 Hz, 1H, H-4). **$^{13}$C{$^1$H} NMR** (76 MHz, $CDCl_3$, 213 K): $\delta$ 46.06 (C-10), 51.56 (C-8), 53.22 (C-6), 53.56 (C-9), 54.93 (C-7), 62.36 (C-5), 145.47 (C-2), 148.89 (C-1), 152.43 (C-11). **MS** (APCI+, MeOH): *m/z* (%) 531.17 (15) $[M+H]^+$, 422.14 (100) $[RSb]^+$, 301.24 (35) $[R]^+$. HRMS (APCI+): Calc. for $[C_{24}H_{34}N_4O_2Sb]^+$ 531.17145. Found: 531.16891.

**Synthesis of [2,6-{MeN(CH$_2$CH$_2$)$_2$NCH$_2$}$_2$C$_6$H$_3$]Bi(O$_2$-1,2-C$_6$H$_4$) (15).** Prepared as described for **11** from **2** (0.20 g, 0.34 mmol), catechol (0.04 g, 0.34 mmol) and KOH (0.08 g, 1.36 mmol) in ethanol (25 mL). Work-up of the reaction mixture (see ESI†) gave **15** as a colourless solid (0.07 g, 33%), m.p. 230 °C. **$^1$H NMR** (600 MHz, $CDCl_3$, 295 K): $\delta$ 2.13 (dd, $^2J_{H\text{-}9a,H\text{-}9e} \approx {}^3J_{H\text{-}8a,H\text{-}9a}$ =10.8 Hz, 2H, H-9a), 2.31-2.49 [m, 12H, overlapped resonances for H-6a, H-7e and H-8a with H-10 ($\delta$ 2.37 ppm, s)], 2.71 (d, $^2J_{H\text{-}8a,H\text{-}8e}$ = 11.5 Hz, 2H, H-8e), 2.76 (d, $^2J_{H\text{-}9a,H\text{-}9e}$ = 11.5 Hz, 2H, H-9e), 3.02 (d, $^2J_{H\text{-}7a,H\text{-}7e}$ = 11.1 Hz, 2H, H-7a), 3.37 (d, $^2J_{H\text{-}5a,H\text{-}5e}$ = 13.3 Hz, 2H, H-5e), 3.80 (d, $^2J_{H\text{-}6a,H\text{-}6e}$ = 10.3 Hz, 2H, H-6e), 4.54 (d, $^2J_{H\text{-}5a,H\text{-}5e}$ = 13.3 Hz, 2H, H-5a), 6.28-6.32 (m, AA′BB′ vicinal spin system, 2H, H-13), 6.45-6.49 (m, AA′BB′ vicinal spin system, 2H, H-12), $A_2B$ spin system with B at $\delta$ 7.23 ppm (t, $^3J_{H\text{-}3,H\text{-}4}$ = 7.4 Hz, 1H, H-4) and A at $\delta$ 7.37 ppm (d, $^3J_{H\text{-}3,H\text{-}4}$ = 7.4 Hz, 2H, H-3). **$^{13}$C{$^1$H} NMR** (151 MHz, $CDCl_3$, 297 K): $\delta$ 46.10 (C-10), 51.58 (C-8), 53.55 (C-6), 54.89 (C-9), 56.53 (C-7), 64.23 (C-5), 116.87 (C-13), 118.43 (C-12), 128.50 (C-3), 128.98 (C-4), 150.26 (C-2), 156.72 (C-11), 198.77 (C-1). **MS** (APCI+, MeOH): *m/z* (%) 619.25 (37) $[M+H]^+$, 510.22 (83) $[M–O_2C_6H_4]^+$, 303.25 (50), $[R+2H]^+$. HRMS (APCI+): Calc. for $[C_{24}H_{34}BiN_4O_2]^+$ 619.24801, Found: 619.24712.

## Conclusions

Clear and general synthetic protocols for new well-defined hypervalent, organometallic compounds of heavy pnicogens [Sb(III), Bi(III)] with a new pincer group, 2,6-[MeN(CH$_2$CH$_2$)$_2$NCH$_2$]$_2$C$_6$H$_3$, and various oxo ligands (oxido, hydroxo, carbonato, 1,2-diolato) are reported. The first molecular structures of 2-organo-1,3,2-dioxastibolanes/bismolanes and -stiboles/bismoles were established by single-crystal X-ray diffraction. The stabilization by intramolecular coordination of **10** and **11** evaluated by theoretical methods is smaller than in related compounds with T-shaped geometry, as **1** or **2**. DFT calculated Gibbs free energies of **8**-**15** showed that the formation of the organopnicogen chelates is better favoured when the OH functionalities of the 1,2-dihydroxy compounds are more acidic. The compounds reported here might be used as trapping agents for gaseous $CO_2$ in mild conditions as shown for the oxides *cyclo*-[2,6-{MeN(CH$_2$CH$_2$)$_2$NCH$_2$}$_2$C$_6$H$_3$]$_2$M$_2$O$_2$ [M = Sb (**3**), Bi (**4**)] which gave "RMCO$_3$" [M = Sb (**6**), Bi (**7**)]. This type of reactivity as well as the potential catalytic activity in reactions which involve $CO_2$ activation is currently investigated for the other organopnicogen(III) species reported here. An important fact is also the experimental observation of water hexamer cluster with a [tetramer+2] motif in the crystal of the oxide **4**·4H$_2$O.

## Acknowledgements

Financial support from National Research Council of Romania (CNCS, Research Project No. PN-II-ID-PCE-2011-3-0933) is greatly appreciated. A.P. thanks Babeş-Bolyai University for a GTC-34054/2013 fellowship. The support provided by Augustin Mădălan (University of Bucarest, Romania), Alexandra Pop and Albert Soran (NATIONAL CENTER FOR X-RAY DIFFRACTION, Babeş-Bolyai University, Cluj-Napoca, Romania) for the solid state structure determinations is highly acknowledged.

## Notes and references

Departamentul de Chimie, Centrul de Chimie Supramoleculară Organică şi Organometalică (CCSOOM), Facultatea de Chimie şi Inginerie Chimică, Universitatea Babeş-Bolyai, 400028 Cluj-Napoca, Romania.

† Electronic Supplementary Information (ESI) available: detailed synthetic procedures for compounds **12**-**15**; NMR spectra; X-ray crystallographic data in CIF format for **1**, **3**, **4**·4H$_2$O, **5**·H$_2$O·C$_6$H$_5$Me, **8**·H$_2$O, **10**·2H$_2$O, **11**·2H$_2$O, **12**, **14** and **15**; figures representing the optical isomers as well as the supramolecular architectures in the crystals of these compounds; cartesian coordinates and graphical representations of all the optimized structures in *xyz* format; representations of the overlapped calculated and crystallographically determined molecular structures. See DOI: 10.1039/b000000x/

‡ *Dedicated to Professor Hans Joachim Breunig (Universität Bremen, Germany) on the occasion of his 70$^{th}$ birthday.*

1 C. I. Raţ, C. Silvestru and H. J. Breunig, *Coord. Chem. Rev.*, 2013, **257**, 818.
2 H. J. Breunig, L. Königsmann, E. Lork, N. Philipp, M. Nema, C. Silvestru, A. Soran, R. A. Varga and R. Wagner, *Dalton Trans.*, 2008, 1831.
3 S.-F. Yin, J. Maruyama, T. Yamashita, S. Shimada, *Angew. Chem. Int. Ed.*, 2008, **47**, 6590.
4 L. Dostál, R. Jambor, A. Růžička, M. Erben, R. Jirásko, E. Černošková and J. Holeček, *Organometallics*, 2009, **28**, 2633.
5 D. R. Kindra, I. J. Casely, M. E. Fieser, J. W. Ziller, F. Furche and W. J. Evans, *J. Am. Chem. Soc.*, 2013, **135**, 7777.
6 R. Nomura, A. Ninagawa and H. Matsuda, *J. Org. Chem.*, 1980, **45**, 3735.
7 R. Nomura, Y. Hasegawa, M. Ishimoto, T. Toyosaki and H. Matsuda, *J. Org. Chem.*, 1992, **57**, 7339.
8 S.-F. Yin and S. Shimada, *Chem. Commun.*, 2009, 1136.
9 R. Qiu, Z. Meng, S. Yin, X. Song, N. Tan, Y. Zhou, K. Yu, X. Xu, S. Luo, C.-T. Au and W.-Y. Wong, *ChemPlusChem*, 2012, **77**, 404.
10 D. R. Kindra and W. J. Evans, *Dalton Trans.*, 2014, **43**, 3052.

11 I. J. Casely, J. W. Ziller, M. Fang, F. Furche and W. J. Evans, *J. Am. Chem. Soc.*, 2011, **133**, 5244.
12 T. A. Hanna, A. L. Rieger, P. H. Rieger and X. Wang, *Inorg. Chem.*, 2002, **41**, 3590.
13 T. A. Hanna, *Coord. Chem. Rev.*, 2004, **248**, 429.
14 M. Mehring, *Coord. Chem. Rev.*, 2007, **251**, 974.
15 X. Kou, X. Wang, D. Mendoza-Espinosa, L. N. Zakharov, A. L. Rheingold, W. H. Watson, K. A. Brien, L. K. Jayarathna and T. A. Hanna, *Inorg. Chem.*, 2009, **48**, 11002.
16 D. A. Atwood, A. H. Cowley and J. Ruiz, *Inog. Chim. Acta*, 1992, **198**, 271.
17 A. P. Soran, C. Silvestru, H. J. Breunig, G. Balazs and J. C. Green, *Organometallics*, 2007, **26**, 1196.
18 M. Wieber and N. Baumann, *Z. Anorg. Allg. Chem.*, 1973, **402**, 43.
19 N. Baumann and M. Wieber, *Z. Anorg. Allg. Chem.*, 1974, **408**, 261.
20 M. Wieber and N. Baumann, *Z. Anorg. Allg. Chem.*, 1975, **418**, 167.
21 Z. Benmaarouf, P. Riviere, M. Rivièbre-Baudet, A. Castel, A. Khallaayoun and M. Ahbala, *Phosphorus, Sulfur Silicon Relat. Elem.*, 1997, **128**, 19.
22 M. Wieber and U. Baudis, *Z. Anorg. Allg. Chem.*, 1976, **423**, 40.
23 A. Soran, H. J. Breunig, V. Lippolis, M. Arca and C. Silvestru, *Dalton Trans.*, 2009, 77.
24 H. J. Breunig, M. G. Nema, C. Silvestru, A. P. Soran and R. A. Varga, *Dalton Trans.*, 2010, **39**, 11277.
25 J. F. C. Boodts and W. A. Bueno, *J. Chem. Soc., Faraday Trans. 1*, 1980, **76**, 1689.
26 F. Huber, T. Westhoff and H. Preut, *J. Organomet. Chem.*, 1987, **323**, 173.
27 L. M. Opris, A. Silvestru, C. Silvestru, H. J. Breunig and E. Lork, *Dalton Trans.*, 2004, 3575.
28 A. M. Preda, C. I. Raţ, C. Silvestru, H. J. Breunig, H. Lang, T. Rüffer and M. Mehring, *Dalton Trans.*, 2013, **42**, 1144.
29 M Chovancová, R. Jambor, A. Růžička, R. Jirásko, I. Císařová and L. Dostál, *Organometallics*, 2009, **28**, 1934.
30 J. Emsley, *Die Elemente*, Walter de Gruyter, Berlin, 1994.
31 Dostál, R. Jambor, A. Růžička, R. Jirásko, I. Císařová and J. Holeček, *J. Fluorine Chem.*, 2008, **129**, 167.
32 A. Fridrichová, T. Svoboda, R. Jambor, Z. Padělková, A. Růžička, M. Erben, R. Jirásko and L. Dostál, *Organometallics*, 2009, **28**, 5522.
33 *IUPAC Nomenclature of Organic Chemistry*, Pergamon Press, Oxford, 1979.
34 D. Copolovici, V. R. Bojan, C. I. Raţ, A. Silvestru, H. J. Breunig and C. Silvestru, *Dalton Trans.*, 2010, **39**, 6410.
35 N. Tokitoh, Y. Arai, T. Sasamori, R. Okazaki, S. Nagase, H. Uekusa and Y. Ohashi, *J. Am. Chem. Soc.*, 1998, **120**, 433.
36 T. Sasamori, Y. Arai, N. Takeda, R. Okazaki, Y. Furukawa, M. Kimura, S. Nagase and N. Tokitoh, *Bull. Chem. Soc. Jpn.*, 2002, **75**, 661.
37 H. J. Breunig, M. A. Mohammed and K. H. Ebert, *Z. Naturforsch., Teil B*, 1994, **49**, 877.
38 *Nomenclature of Inorganic Chemistry–IUPAC Recommendations 2005*, ed. N. G. Connelly, T. Damhus, R. M. Hartshorn and A. T. Hutton, RSC Publishing, Cambridge, 2005.
39 G. Hincapié, N. Acelas, M. Castaño, J. David and A. Restrepo, *J. Phys. Chem. A*, 2010, **114**, 7809.
40 R. Ludwig, *Angew. Chem., Int. Ed.*, 2001, **40**, 1808.
41 C. Pérez, M. T. Muckle, D. P. Zaleski, N. A. Seifert, B. Temelso, G. C. Shields, Z. Kisiel and B. H. Pate, *Science*, 2012, **336**, 897.
42 M. Nishio, *Phys. Chem. Chem. Phys.*, 2011, **13**, 13873.
43 L. Goerigk and S. Grimme, *Phys. Chem. Chem. Phys.*, 2011, **13**, 6670.
44 G. R. Fulmer, A. J. M. Miller, N. H. Sherden, H. E. Gottlieb, A. Nudelman, B. M. Stoltz, J. E. Bercaw and K. I. Goldberg, *Organometallics*, 2010, **29**, 2176.
45 MestReC and MestReNova, Mestrelab Research S.L., A Coruña 15706, Santiago de Compostela.
46 Qual Browser Thermo Xcalibur, version 2.1.0 SP1.1160; Thermo Fischer Scientific Inc.: Waltham, MA, 02454, 2011.
47 A. Altomare, G. Cascarano, C. Giacovazzo, A. Guagliardi, M. C. Burla, G. Polidori and M. Camalli, *J. Appl. Cryst.*, 1994, **27**, 435.
48 G. M. Sheldrik, *Acta Crystallogr., Sect. A: Fundam. Crystallogr.*, 2008, **64**, 112.
49 G. M. Sheldrick, *Acta Crystallogr., Sect. A: Found. Crystallogr.*, 2013, **69**, s74.
50 A. Spek, *Acta Crystallogr., Sect. D: Biol. Crystallogr.*, 2009, **65**, 148.
51 *DIAMOND-Visual Crystal Structure Information System*, Crystal Impact: Postfach 1251, D-53002 Bonn, Germany, 2001.
52 F. Neese, *WIREs Comput. Mol. Sci.*, 2012, **2**, 73.
53 A. D. Becke, *Phys. Rev. A: At., Mol., Opt. Phys.*, 1988, **38**, 3098.
54 E. van Lenthe, E. J. Baerends and J. G. Snijders, *J. Chem. Phys.*, 1993, **99**, 4597.
55 E. van Lenthe, E. J. Baerends and J. G. Snijders, *J. Chem. Phys.*, 1994, **101**, 9783.
56 E. van Lenthe, R. van Leeuwen, E. J. Baerends and J. G. Snijders, *Int. J. Quantum Chem.*, 1996, **57**, 281.
57 S. Grimme, J. Antony, S. Ehrlich and H. Krieg, *J. Chem. Phys.*, 2010, **132**, 154104.
58 S. Grimme, S. Ehrlich and L. Goerigk, *J. Comput. Chem.*, 2011, **32**, 1456.
59 D. A. Pantazis, X.-Y. Chen, C. R. Landis and F. Neese, *J. Chem. Theory Comput.*, 2008, **4**, 908.
60 D. Pantazis and F. Neese, *Theor. Chem. Acc.*, 2012, **131**, 1292.



 